

國 立 交 通 大 學

電 信 工 程 學 系

博 士 論 文

立體超緊耦合結構之研究與其在寬頻耦合器與
帶通濾波器的應用



Three-Dimensional Extremely Tight Coupling
Structures and Their Application on Broadband
Coupler and Bandpass Filter

研 究 生：陳 慧 謹 (Hui-Chun Chen)

指 導 教 授：張 志 揚 (Chi-Yang Chang)

中 華 民 國 九 十 七 年 一 月

立體超緊耦合結構之研究與其在寬頻耦合器與
帶通濾波器的應用

Three-Dimensional Extremely Tight Coupling Structures
and Their Application on Broadband Coupler and
Bandpass Filter

研究生：陳慧諄

Student: Hui-Chun Chen

指導教授：張志揚 博士

Advisor: Dr. Chi-Yang Chang

國立交通大學



A Dissertation

Submitted to Institute of Communication Engineering
College of Electrical and Computer Engineering
National Chiao Tung University
in Partial Fulfillment of the Requirements
for the Degree of Doctor of Philosophy
in
Communication Engineering
Hsinchu, Taiwan

2008 年 1 月

立體超緊耦合結構之研究與其在寬頻耦合器與帶通濾波器的應用

學生：陳慧諄

指導教授：張志揚 博士

國立交通大學

電信工程學系

摘要

本論文主要在研究立體超緊耦合結構，以及其在寬頻耦合器與帶通濾器上的應用。其中所提的二種新型立體超緊耦合結構是一種在兩旁有介質方塊的垂直基板平面電路結構。運用所提此二種耦合結構，我們可以解決實現超寬頻多節串接式混成器所面臨的超緊耦合量、奇偶模模態速度不等與不連續接面等挑戰。在適當的設計之下，我們可以實現一個效能極佳的超寬頻混成器。經由進一步的變化，我們提出並且分析另外二種濾波器結構分別是垂直基板平面電路步階阻抗諧振器與懸置基板帶線步階阻抗諧振器。此二種諧振器所構成的帶通濾波器結構可以實現濾波器具有寬的通帶頻寬(大於二比一)、好而且寬的上止帶表現但是只須要使用一般的印刷電路板製程技術。對於所提結構有詳細的特性敘訴與分析，並且介紹系統化的設計流程以及其在實例上的驗證。

Three-Dimensional Extremely Tight Coupling Structures and Their Application on Broadband Coupler and Bandpass filter

Student: Hui-Chun Chen Advisor: Dr. Chi-Yang Chang

Department of Communication Engineering
National Chiao Tung University

Abstract

This dissertation presents the research and applications of three-dimensional extremely tight coupling structures. Two of them are the modified vertically installed planar structures with dielectric block at both side of vertical substrate. With these two newly proposed structures, we have overcome the three main challenges in realization of ultra-broadband multi-section quadrate hybrid. The challenges are to obtain an extremely tight coupling value, to compensate the unequal even- and odd-mode modal phase velocitys, and to minimize the discontinuous effect at junctions. Thanks to the proposed structures a five-section ultra-broadband quadrate hybrid with excellent performance is realized. Extending the application of tight coupling structures to broadband filters, two stepped impedance resonator (SIR) structures are proposed. The proposed SIR structures are the vertically installed planar stepped impedance resonator (VIPSIR) and the suspended substrate stripline stepped impedance resonator (SSSSIR). These two filter structures can realize bandpass filters with broad passband of larger than 1:2, good and wide upper stopband performance. More importantly, conventional PCB process can be applied to mass produce

both filters. The analysis procedures and the characteristics of the proposed structures are described in detail. Moreover, systematical design procedures are given and proved to be valid with several experimental examples in this dissertation.



謝誌

首先要感謝張志揚教授在這六年多辛勤與耐心的指導，每當我陷入研究的困境時都能適時的激勵、啟發與指正，帶我走出迷惘，也使得本論文可以完成。另外也感謝口試委員鍾世忠教授、林育德教授、郭仁財教授、邱煥凱副教授與湯敬文副教授對於本論文研究所給予的指正與意見。

這裡也要感謝微波實驗室的學長、弟、妹們多年的照顧。特別是正中、士鳴、竟谷與鈞翔在此其間所給與的意見與鼓勵。最後在此感謝我的家人、妻子、同事在此期間對我的支持與鼓勵。



慧諱

2008年一月於台灣新竹

Contents

Abstract (Chinese).....	I
Abstract.....	II
Acknowledgement.....	III
Contents.....	IV
List of Tables.....	VI
List of Figures.....	VII
1 Intorduction	1
1.1 Coupled structures.....	2
1.2 Motivation.....	5
1.3 Chapter outline.....	9
2 Analysis and Characteristic of Proposed Structure	10
2.1 Analysis and characteristic of proposed modified VIP coupled lines.....	10
2.2 Structures of proposed VIPSIR and SSSSIR.....	14
2.3 Analysis and characteristic of proposed filter structure.....	16
2.4 Characteristics of filter structure A.....	16
2.5 Characteristics of filter structure B.....	20
3 Analysis, Design and Realization of Ultra-Broadband Multi-Section Quadrature Hybrid	25
3.1 Literature survey.....	25
3.2 Theory and design procedures.....	26

3.3 Ultra-broadband multi-section quadrature hybrid using modified VIP coupler.....	31
4 Analysis, Design and Realization of Broadband Bandpass Filters with Wide Upper Stopband Using Parallel-coupled VIPSIRs and SSSIRs.....	34
4.1 Literature survey.....	34
4.2 Filter design procedures.....	36
4.3 Simulation and measurement.....	38
4.4 Simulation and measurement using VIPSIR.....	38
4.5 Simulation and measurement using SSSIR.....	43
5 Conclusions.....	45
Reference.....	47



List of Tables

Table 3.1 Design parameters and physical dimensions of experimental coupler.....	31
Table 4.1 Specifications and dimensions of the experimental filters of structure A.....	38
Table 4.2 Specifications and dimensions of the experimental filters of Filter structure B.....	43



List of Figures

Fig. 1.1 Edged-coupled microstrip lines (a) cross-sectional view (b) top view.....	3
Fig. 1.2 Enhanced edge-coupled structures of (a)-(b) re-entrant coupled lines and (c)-(d) Lange coupler.	4
Fig. 1.3 Broadside coupled transmission: (a) Broadside coupled suspended microstrip lines. (b) Offset broadside coupled suspended microstrip lines.....	4
Fig. 1.4 Cross-sectional view of a conventional VIP coupling structure.....	5
Fig. 1.5 Three-dimensional view of proposed modified VIP structure coupling structures (a) type I with dielectric overlays for moderate coupling, and (b) type II with dielectric overlays and finite-extent ground plan for extremely tight coupling.....	7
Fig. 1.6 The proposed filter resonator structures. (a) Structure A use the vertically installed planar stepped impedance resonator, and (b) structure B adopts the suspended substrate stripline stepped impedance resonator (SSSSIR).....	8
Fig. 2.1 Cross-sectional views of (a) type I, and (b) type II of the modified VIP couplers, where $H_{sub}=0.508mm$, $W_{VIP}=0.2032mm$, $H_{VIP}=3.048mm$, $W_{DR}=5.08mm$, $W_{gnd}=0.381mm$, $H_{DR}=1.524mm$, and $\epsilon_{r1}=\epsilon_{r2}=\epsilon_{r3}=3.38$	11
Fig. 2.2 Even- and odd-mode characteristic impedances versus VIP metal height (H_{metal}) of the type I VIP coupler with (a) $G=0.4572mm$, and (b) $G=0.7112mm$	12
Fig. 2.3 (a) even- and odd-mode characteristic impedances, and (b) effective dielectric constants versus G_{gnd} and H_{metal} of the type II VIP coupler.....	13
Fig. 2.4 The proposed filter structures. (a) Structure A where the vertically installed planar stepped-impedance resonators are used, and (b) structure B where the modified stripline stepped-impedance resonators are used.....	14
Fig. 2.5 Equivalent circuit for structure A and B in Fig. 2.4, where P-P' is the symmetrical plane.....	15

Fig. 2.6 Cross-sectional views of filter structure A. (a) vertically installed planar-coupled line, and (b) high impedance uncoupled line, where $H_{sub}=0.508\text{mm}$, $H_{VIP}=0.2032\text{mm}$, $W_{HZ}=0.254\text{mm}$, $W_{VIP}=3.048\text{mm}$, and $\epsilon_{r1}=\epsilon_{r2}=3.38$ are chosen in this paper.....17

Fig. 2.7 (a) Even-mode and (b) Odd-mode characteristic impedances versus strip width (W_{LZ}) on the vertical substrate with various patch width (W) on the main substrate, where $H_{sub}=0.508\text{mm}$, $H_{VIP}=0.2032\text{mm}$, $W_{HZ}=0.254\text{mm}$, $W_{VIP}=3.048\text{mm}$, and $\epsilon_{r1}=\epsilon_{r2}=3.38$18

Fig. 2.8 (a) Even-mode and (b) Odd-mode effective dielectric constants versus strip width (W_{LZ}) on the vertical substrate with various patch width (W) on the main substrate, where $H_{sub}=0.508\text{mm}$, $H_{VIP}=0.2032\text{mm}$, $W_{HZ}=0.254\text{mm}$, $W_{VIP}=3.048\text{mm}$, and $\epsilon_{r1}=\epsilon_{r2}=3.38$19

Fig. 2.9 Effective dielectric constant and characteristic impedance versus the distance (D_{HZ}) between high impedance line and the main substrate where the strip width W_{HZ} on the vertical substrate is fixed to be 0.254mm, $H_{sub}=0.508\text{mm}$, $H_{VIP}=0.2032\text{mm}$, $W_{VIP}=3.048\text{mm}$, and $\epsilon_{r1}=\epsilon_{r2}=3.38$20

Fig. 2.10 Cross-sectional views of the filter structure B. (a) broadside-coupled line, and (b) high impedance uncoupled line, where $H_1=0.508\text{mm}$, $H_2=0.2032\text{mm}$, $W_{HZ}=0.2032\text{mm}$, $\epsilon_{r1}=\epsilon_{r2}=3.38$, and P-P' is the symmetrical plane.....21

Fig. 2.11 (a) Even-mode and (b) Odd-mode characteristic impedances versus ground plane aperture size (G_{gnd}) with various broadside coupled-line width (W), where $H_1=0.508\text{mm}$, $H_2=0.2032\text{mm}$, $W_{HZ}=0.2032\text{mm}$, and $\epsilon_{r1}=\epsilon_{r2}=3.38$22

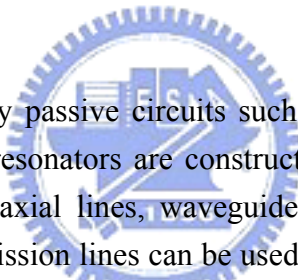
Fig. 2.12 (a) Even-mode and (b) Odd-mode effective dielectric constants versus ground plane aperture size (G_{gnd}) with various broadside coupled-line widths (W), where $H_1=0.508\text{mm}$, $H_2=0.2032\text{mm}$, $W_{HZ}=0.2032\text{mm}$, and $\epsilon_{r1}=\epsilon_{r2}=3.38$23

Fig. 2.13 Effective dielectric constant and characteristic impedance versus the ground plane aperture size (G_{gnd}), where $H_1=0.508\text{mm}$, $H_2=0.2032\text{mm}$, $W_{HZ}=0.2032\text{mm}$, and

$\epsilon_{r1}=\epsilon_{r2}=3.38$	24
Fig. 3.1 Schematic circuit representation of a single-section coupler.....	26
Fig. 3.2 Schematic circuit expression of coupler with (a) even mode excitation and (b) odd mode excitation.....	27
Fig. 3.3 A N-section cascaded symmetrical quadrature hybrid.....	29
Fig. 3.4 Photograph of the fabricated five-section 3dB directional coupler.....	31
Fig. 3.5 Simulated responses of the proposed hybrid.....	32
Fig. 3.6 Measured responses of the proposed hybrid.....	32
Fig. 3.7 Measured and simulate amplitude and phase errors of the proposed hybrid.....	33
Fig. 4.1 Simulated and measured responses of filter A.....	39
Fig. 4.2 Simulated and measured responses of filter B.....	40
Fig. 4.3 A sketch drawing for filter D. A high impedance microstrip line is used to connect two VIP substrates. The numbers on the mail substrate indicate the section number in Table 4.1.....	40
Fig. 4.4 Simulated and measured responses for filter C.....	41
Fig. 4.5 Simulated and measured responses for filter D.....	42
Fig. 4.6 Photographs of proposed (a) filter A and (b) filter B.....	42
Fig. 4.7 Simulated and measured responses of filter A.....	44
Fig. 4.8 Simulated and measured responses of filter B.....	44
Fig. 4.9 Photographs of fabricated (a) filter E and (b) filter F.....	44

Chapter 1

Introduction



In microwave systems, many passive circuits such as impedance transformers, filters, couplers, dc blocks, baluns, and resonators are constructed by distributed type coupled and uncoupled transmission lines. Coaxial lines, waveguides, strip lines, microstrip lines, and many other types of planar transmission lines can be used to realize the mentioned circuits. In the past few decades, microstrip coupled lines are widely used and have been deeply studied due to their low cost, suitability for circuit integration, and ease of fabrication. However, it is still a challenge to design and implement some key components by microstrip line. For instance, an ultra-broadband multi-section 3dB quadrature hybrid, and a broadband coupled-line filter are both not easy to implement by microstrip line. However, these broadband circuits become more and more important in the modern broadband wireless communication system. For the multi-section 3-dB hybrid, an extremely tight coupled line with coupling of -0.8dB is required, but is hard to realize by the PCB etching technology. Although a broadside stripline coupling structure or a Lange type interdigital coupler configuration can realize relatively tight coupling (the Lange coupler can realize coupler only to about -3dB), the broadside coupling structure needs a complex mechanical housing whereas the Lange coupler requires a high dielectric constant substrate and some bounding wires. They are both costly and not suitable for commercial high-volume production. In this dissertation we propose several three-dimensional coupling structures which are not only easy to realize extremely tight coupled lines by low dielectric constant substrates but also suitable for conventional printed circuit board (PCB) fabrication processes. Furthermore, the proposed tight coupling structures can also implement broadband coupled-line filters. Detailed analysis

of each proposed configuration is presented in chapter 2. In this chapter, we will summarize various types of existing coupled-line structure, describe research motivation, discuss proposed structures, and give an outline of this dissertation.

1.1 Coupled Structures

When two unshielded transmission lines are placed close to each other, a portion of the power presented on the first line will couple to the second line. The closer the lines are placed, the stronger the coupling takes place. The coupled power on the second line is not only a function of the physical dimensions of the structure but also a function of operation frequency and the propagation mode. Moreover, coupled-line structures can be of any forms and using different types of transmission lines, depending on the demanded application and performance. According to the coupling strength, it can be briefly divided into loosely ($<-20\text{dB}$), moderate ($<-8\text{dB}$), tight ($>-3\text{dB}$), and extremely tight ($>-1\text{dB}$) couplings. Various types of coupling structures with different types of transmissions have different inherent coupling strength which is suitable for different applications of circuits. It is summarized in the following section. In general microwave circuits such as multi-section coupler, and bandpass filters are constructed by various coupled lines with different coupling strength. Also, as the operation bandwidth of coupler becomes wider the coupling strength between different coupled sections will also change accordingly. In some cases, the abrupt change between two sections causes strong discontinuities which should also be considered to achieve wanted circuit performances.

Several distinct types of coupled line have been studied. According to the coupling mechanism, they could be categorized in three distinct coupling structures which are edge-coupled, enhanced edge-coupled, and broadside-coupled. These will be discussed in detail in the followings.

The most commonly used coupled-line structures is edge-coupled structure as shown in Fig. 1.1 [1] in which the electromagnetic field interact between coupled lines are only take place on the inner edge of transmission lines. Therefore, the closer of the coupled lines the stronger the coupling strength we can get. Usually, microstrip coupled lines, and microstrip-like lines such as inverted microstrip lines, suspendend microstrip lines, and coplanar waveguide can easily implement these kinds of edge-coupled structures. However, these coupled lines are only suitable for loosely to moderate coupling strength due to practical spacing limitation between two lines in PCB etching process. Edge-coupled structures in microstrip line configuration are planar type, easy to integrate with other circuits, suitable for low cost PCB implementation, and having well developed design formulations. Therefore, it is widely used in many RF and microwave circuits such as loose coupler, narrow band bandpass filters, and DC blocks. However, as the required coupling getting tighter, it becomes

more difficult in practical implementations. Moreover, due to the propagation wave is quasi-TEM mode in microstrip structure, the odd mode phase velocity is faster than the even mode. The unequal modal phase velocity causes poor directivity which degrades some circuit performances.

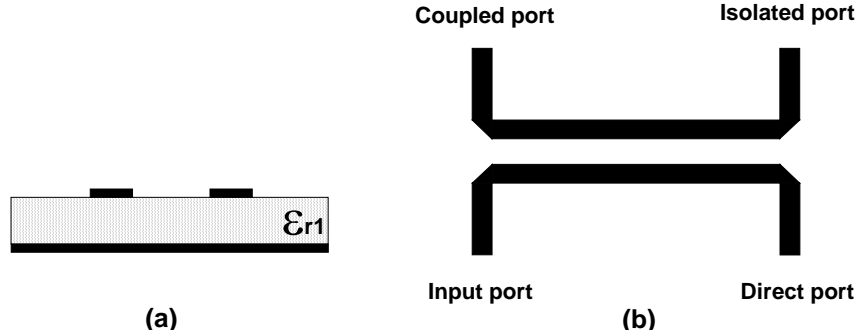


Fig. 1.1 Edged-coupled microstrip lines (a) cross-sectional view (b) top view.

To overcome the described problems, some coupling structures were proposed which can be categorized as enhanced edge-coupled structures. Fig. 2(a) and (b) show the re-entrant structure [2], Fig. 2(c) and (d) depict the interdigital Lange coupler [3]. Those are two of the most commonly used enhanced edge-coupled structures. Enhanced edge-coupled structures maintain the coupling mechanism of edge-coupled lines and keep the advantages of planar type structure. More importantly, the coupling strength is improved significantly compared to conventional edge-coupled lines. The re-entrant design can largely reduce the odd-mode impedance by introducing the third metal and still keeps the high even-mode impedance. Besides, by properly adjusting the width of the third metal and thickness and dielectric constant of the substrate, the unequal modal phase velocities can be compensated. The Lange coupler combines interdigital arranged strip pairs with air bridges or wire bonding which can increase the odd-mode capacitance. However, these kinds of enhanced edge-coupled structures can realize tight coupling only by use of substrate with related high dielectric constant which is expensive and rarely used in volume production. Further more, extra wire bonding process in the Lange coupler induce parasitic inductance which need tuning back and forth during implementation.

Another popular coupled structure usually been adapted to broadband circuit is broadside coupling structures [4]. Fig. 1.3 shows its cross sectional view. In Fig.3, usually three layers of substrates are used. However, if the top layer and bottom layer are air, the structure is so-called suspended substrate broadside coupler. In broadside coupling structure, the odd-mode capacitance involves almost entire overlapping areas. Therefore, increasing the overlapping areas, we can easily achieve a very tight coupling. Unfortunately, the modal phase velocity is usually quite different in suspend substrate broadside coupler. To overcome this, the stripline structure where the three layers of substrate are with the same dielectric

constant is usually adopted. Although broadside coupling in strip line structure can realize an ideal coupler with wide coupling range, these stripline structures usually require special mechanical housing to support it which is complex and need precisely assembly procedures. Moreover, the well known drawback of a conventional stripline is that it is much more difficult to integrate with passive and active components than its microstrip counterpart is.

A detail history of research on microwave directional couplers including various types of coupling structures and an extensive reference list is given by Cohn and Levy [5].

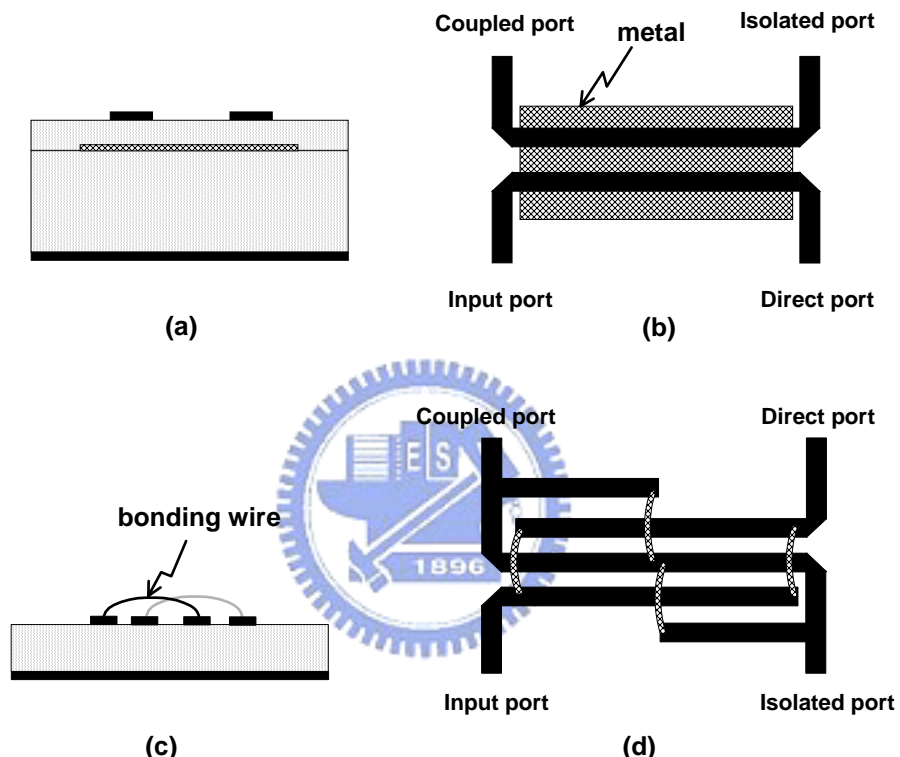


Fig. 1.2 Enhanced edge-coupled structures of (a)-(b) re-entrant coupled lines and (c)-(d) Lange coupler.

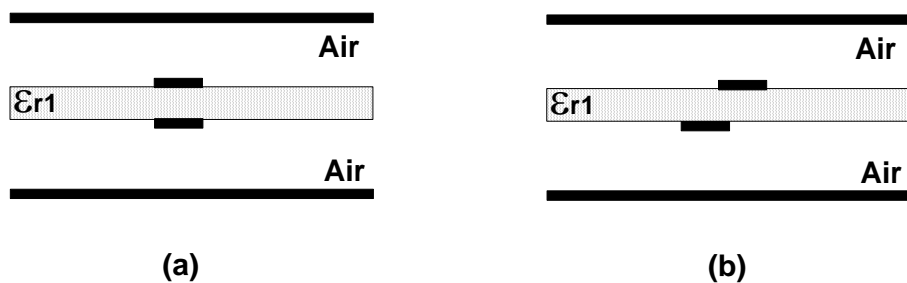


Fig. 1.3 Broadside coupled transmission: (a) Broadside coupled suspended microstrip lines. (b) Offset broadside coupled suspended microstrip lines

1.2 Motivation

Microstrip lines have been widely used in microwave circuits due to its high level integration of both active and passive components. In several applications such as balanced amplifiers, balanced mixers, etc, a tight coupling of 3dB or more is required. However, the parallel coupled microstrip line is difficult to fulfill the demand of tight coupling strength due to the limitation photo-etching technology. This limitation is also a main challenge to realize a microstrip broadband parallel-coupled filter.

The vertically installed planar (VIP) coupled line as shown in Fig. 1.4 was first proposed by Awai [6]. The VIP circuit consists of a broadside coupled line which is vertically soldered with the microstrip line on the main substrate. This VIP coupled line structure can easily achieve a coupling tighter than 3dB. In the mean time, it encounters a serious unequal modal phase velocities. It is the reason why there is no multi-section cascade quadrature hybrid being reported with the conventional VIP coupled lines up to the time of this study.

Quadrature hybrid is one of the key elements in many microwave circuits such as balanced amplifier, balanced mixer, phase shifter, power divider, and beam-forming network for array antennas and for direction-finding antennas. Nowadays, ultra-broadband performance with low cost PCB process is demanded in many applications. It is well known that the most common way to realize a 3dB quadrature coupler with multi-octave bandwidth is to cascade of several quarter-wave coupled line sections. However, there are three challenges in practical realization as described in the following.

First, the central section of the ultra-broad band multi-section quadrature hybrid (3dB) usually requires an extremely tight coupling (greater than -1dB) and still maintain the same modal phase velocity. For example, in a 5 sections 3 dB quadrature coupler with +/- 0.5dB pass band ripple, the coupling strength in the central section is -0.8dB. From our study, the conventional VIP coupled line structure shown in Fig. 1.4 is difficult to realize such kind of extremely tight coupling (-0.8dB) using low cost PCB substrate material which dielectric constant is usually low (3.3 to 4.4 typically).

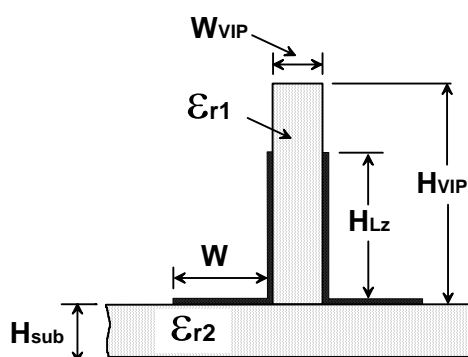


Fig. 1.4 Cross-sectional view of a conventional VIP coupling structure.

Second, although the unequal phase velocities can be compensated by carefully choosing the vertical substrate [7], it is not suitable for the coupling as tight as -0.8dB . Our investigation shows that the unequal even- and odd-mode modal propagation constants slightly degrade the performances of isolation and return loss of a single section 3dB quadrature coupler. However, the unequal modal phase velocities become a disaster on the performances of a multi-section 3dB quadrature coupler. The degradation of the performances includes the equal-ripple coupling, the isolation, and the return loss over its bandwidth. Hence, the modification on the conventional VIP structure is required to overcome the problem.

Finally, when the coupled sections are cascaded, the inner sections of coupled lines always require tighter coupling strength than the outer sections. Therefore, the even- and odd-mode impedances of each section are quite different from those of the adjacent ones. Consequently, the line width of each section abruptly changes at the junction which results in a large discontinuity effect and shows coupling error and directivity degradation. Therefore, to figure out a suitable physical structure of each coupling section that maintains the coupling value but minimizes the discontinuity effect between junctions is very important.

In short, the most challenging works to realize a multi-section quadrature hybrid are achieving of an extremely tightly coupled center section, equalizing of modal phase velocities, and minimizing of the discontinuity effect between each section. In the past, only strip line circuits can solve all of these three problems. However, the conventional stripline circuits encounter the drawbacks described previously.

In this dissertation two newly proposed VIP coupling structures are presented to realize a microstrip multi-section 3dB quadrature hybrid. The proposed structures are suitable for conventional PCB processes. Shown in Fig. 1.5(a) and (b) are the three-dimensional views of two proposed VIP coupling structures which can achieve the mentioned demands. We call the structure in Fig. 1.5(a) the type I and Fig. 1.5(b) the type II VIP coupling structure. The dielectric blocks at both sides of the VIP coupler, which use similar material as the main and VIP substrate. These dielectric blocks are effective to increase the even-mode effective dielectric constant. As a result, the modal phase velocities could be equalized. In the proposed type I VIP coupling structure, there are four metal strips that two of them are on the VIP substrate and the other two are on the main substrate. The strips on the VIP substrate and the strips on the main substrate are connected at two ends and at the center of the coupler. This structure can implement a coupler with coupling from moderate to tight coupling.

The type I VIP coupling structure is impossible to achieve coupling value as tight as -0.8dB even when W equals to 0. To implement the extremely tight-coupled center section for multi-section cascade quadrature hybrid, the type II of modified VIP coupler is proposed as shown in Fig. 5(b). In this Figure, the ground plane in the main substrate changes to two metal strips. Utilizing this finite-extent ground plane (in this case only two ground strips) structure, the VIP coupler can achieve a coupling of tighter than -0.8 dB . Again, a similar dielectric block as the type I is used to compensate the modal phase velocities.

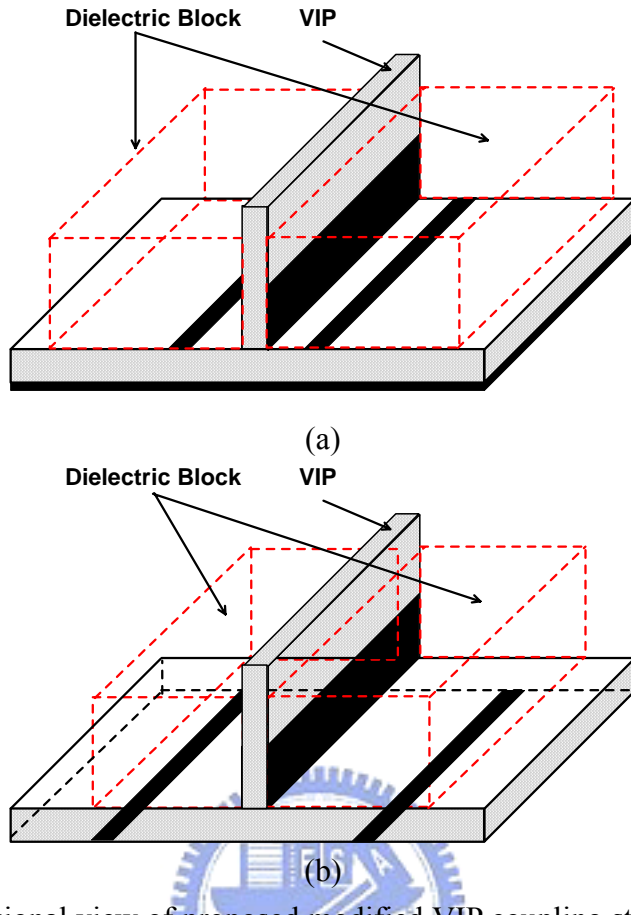


Fig. 1.5 Three-dimensional view of proposed modified VIP coupling structures (a) type I with dielectric overlays for moderate coupling, and (b) type II with dielectric overlays and finite-extent ground plan for extremely tight coupling.

Due to both proposed structures are three-dimensional, various combination of physical dimensions can achieve the same electrical parameters (Z_{0e} , Z_{0o}) for each coupling section. This property provides an extra degree of freedom to overcome the discontinuity effect that occurred at the junctions of two coupling sections.

Except the application in the ultra broadband quadrature hybrid, the broadband filter, usually with a bandwidth of broader than an octave, is another attractive application of the extremely tight coupling structure. Many microwave communication systems, for example the UWB system, require very wide bandwidth to handle numerous data simultaneously. Broadband bandpass filters are always on demand for such wideband systems to prevent noise coming into the systems and to minimize spur signals pouring out from defined spectrum. There are many ways to implement broadband bandpass filters. Each kind of broadband bandpass filter has its own advantages and disadvantages. The benefits and drawbacks of each design will be discussed in more detail in chapter 4. Among these filters, the coupled line filter is one of the most popular methods to implement this kind of filters. The coupled line filters such as parallel coupled filters, interdigital filters, and comb-line filters usually

encounter poor upper stopband problem. The stepped impedance resonator (SIR) [8] technique will be adopted in this dissertation to solve the upper stopband problem. However, due to the requirements of large high to low impedance ratio and broad bandwidth of the filter, the extremely tight coupling structures are required. In this dissertation, two newly proposed broadband SIR filter structures as shown in Fig. 1.6(a) and (b) are introduced.

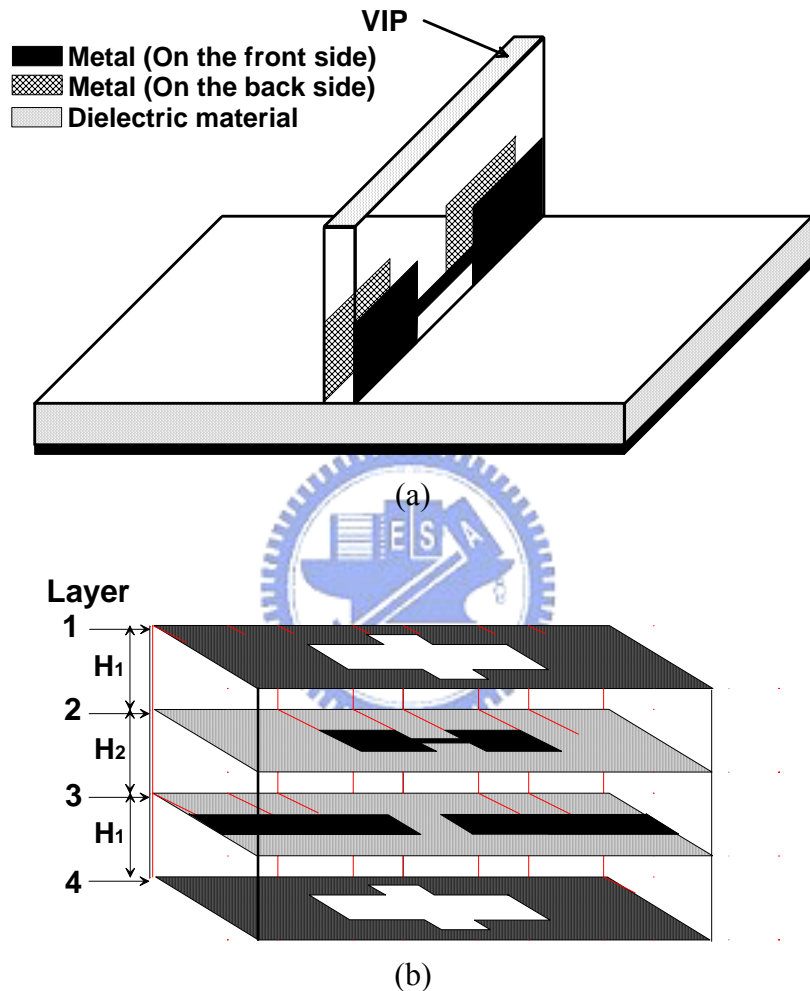


Fig. 1.6 The proposed filter resonator structures. (a) Structure A use the vertically installed planar stepped impedance resonator (VIPSIR), and (b) structure B adopts the suspended substrate stripline stepped impedance resonator (SSSSIR).

Fig. 1.6(a) shows the structure that we call it structure A. In structure A, the vertically installed planar stepped impedance resonators (VIPSIRs) are adopted. In Fig. 1.6(a), the extremely tightly coupled low impedance line section is a vertically installed planar coupler while the very high impedance uncoupled-line section is also implemented on the vertical substrate. The conventional VIP coupling structure shown in Fig. 1.4 has the advantages of simple physical structure, small size, capable of using normal PCB process, and easy to

achieve tight coupling. However, due to the unequal modal phase velocities, only a few applications such as single section 3dB quadrature coupler [6, 7] and filter [9] have been reported using conventional VIP structure. These two applications are both not sensitive to unequal modal phase velocities. However, the filter structure in [9] using VIP uniform impedance resonator (UIR) is a comb-line-like filter structure. The UIR filter usually has poor upper stopband performance. Besides, the comb-line-like structure in [9] is difficult to realize a filter with the order higher than two due to the complex and strong cross coupling effects between different VIP substrates. The proposed VIPSIR filter solves all of the mentioned problems. Although the VIP structure is a three dimensional structure, it can be assembled by a properly designed soldering fixture. As far as we know, the VIP structure has already been used in many mass-produced commercial PCB circuits as a dual band printed inverted-F antenna.

Fig. 1.6(b) depicts the structure B which uses a suspended substrate stepped impedance resonator (SSSSIR). Similar to the structure A, SSSSIR filter also has a tightly-coupled low-impedance coupled-line section and a very high impedance uncoupled-line section. These are implemented in a proposed modified stripline structure where their ground plane has a designed opening. We call it suspended substrate stripline (SSS).

For the coupled-line section, both filter structures can realize a very high even-mode impedance (Z_{0e}), and an extremely low odd-mode impedance (Z_{0o}). For the uncoupled-line section, both structures can implement a very high impedance transmission line. Although Fig. 1.6(a) and (b) show a filter with only one resonator, it can be extended to a filter of any order.

1.3 Chapter Outline.

In this section a brief outline of this dissertation will be given as following. Chapter 1 gives a brief introduction which introduces coupler in different aspect. Chapter 2 describes the proposed two modified VIP coupled line which is suitable for multi-octave equal-ripple 3dB quadrature hybrid in detail. In the same chapter, another two structures that are suitable for implementing broadband bandpass filters with wide upper stopband are also presented. In chapter 3, we introduce the design example of multi-octave equal-ripple quadrature hybrid using proposed modified VIP coupled lines. Several design examples of broadband filters with very wide upper stopband clearance using VIPSIRs and SSSSIRs are presented in chapter 4. The finally conclusion are given in chapter 5.

Chapter 2

Analysis and Characteristic of Proposed Structure

Practical realization of cascaded multi-section quadrature hybrid with multi-octave bandwidth has three challenges. Those are (1) difficult to implement extremely tight coupling, (2) compensate the un-equal modal phase velocities and (3) overcome the junction effects that occur when cascading several coupled sections. Two proposed modified VIP coupled structures as shown in Fig. 1.5 (a) (b) can solve all three challenges. Detail analysis of each structure is presented in section 2.1. In section 2.2, the analysis and characteristics of VIPSIR and SSSSIR which is suitable for implement a broadband filter are described.

2.1 Analysis and Characteristic of Proposed Modified VIP Coupled Lines

The cross-sectional views of proposed modified VIP coupling structures are shown in Fig. 2.1. In order to compensate the unequal modal phase velocities, which is the most challenging work for implementing a VIP coupler, two dielectric blocks are placed at both sides of the VIP coupler. Due to the odd-mode field is bounded within the VIP substrate; the odd-mode modal phase velocity is lower than the even mode. By using the dielectric block with similar material as the main and VIP substrate, more even mode field will pass through the dielectric block. Thus, we can slow down the even-mode phase velocity to equalize it with odd-mode phase velocity. In Fig. 2.1(a), there are four metal strips that two of them are on the VIP substrate and the other two are on the main substrate. The strips on the VIP substrate and the strips on the main substrate are connected at two ends and at the center of the coupler. This structure can implement a coupler with coupling from moderate to tight coupling. The even- and odd-mode characteristic impedances with respect to the VIP metal height (H_{metal})

and the width of the strips on the main substrate (W) are extracted by EM simulation tool HFSS. Fig. 2.2(a)-(b) depicts the extracted even- and odd-mode characteristic data of proposed type I structure, in which the gap width between two strips on the main substrate (G) is 0.4572mm (18mils) and 0.7112mm (28mils) respectively. Observing these curves depicted in Fig. 2.2, the even-mode impedance is mainly decided by the width of the strips on the main substrate (W) while the odd-mode characteristic impedance is mostly controlled by the VIP metal height (H_{metal}). The gap G provides another degree of freedom to choose the total width of the coupler so that the layout of the junction between adjacent sections could have minimal discontinuity.

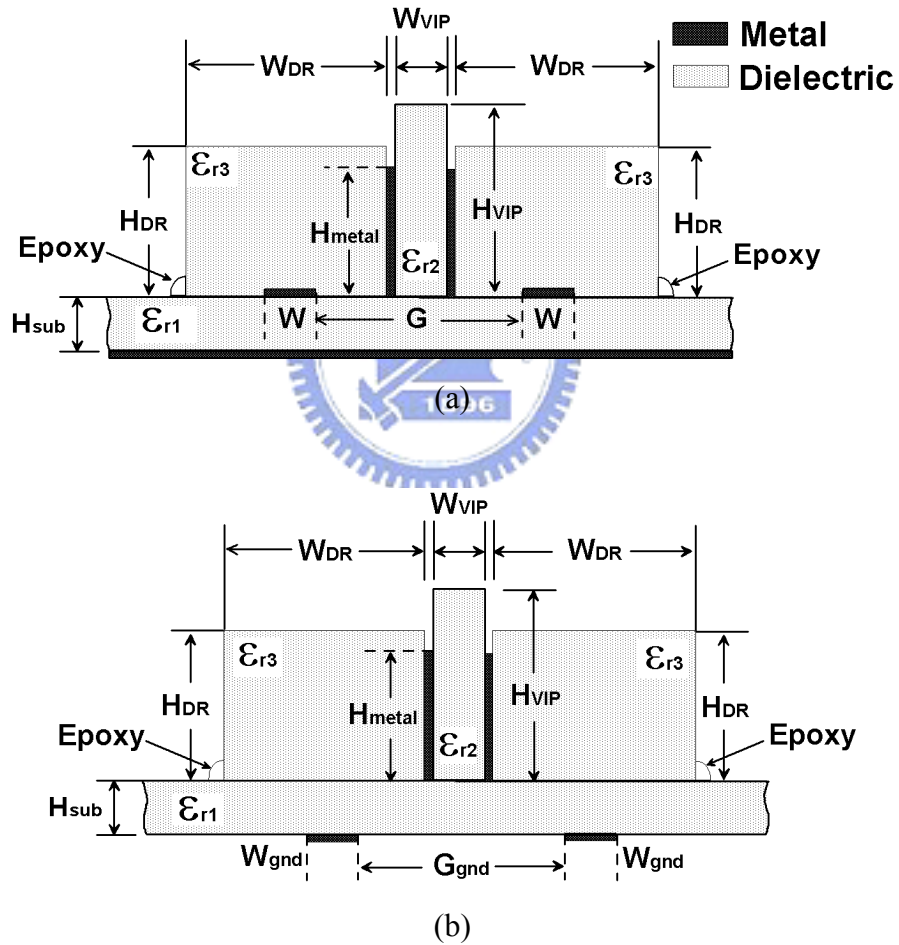


Fig. 2.1 Cross-sectional views of (a) type I, and (b) type II of the modified VIP couplers, where $H_{sub}=0.508\text{mm}$, $W_{VIP}=0.2032\text{mm}$, $H_{VIP}=3.048\text{mm}$, $W_{DR}=5.08\text{mm}$, $W_{gnd}=0.381\text{mm}$, $H_{DR}=1.524\text{mm}$, and $\epsilon_{r1}=\epsilon_{r2}=\epsilon_{r3}=3.38$.

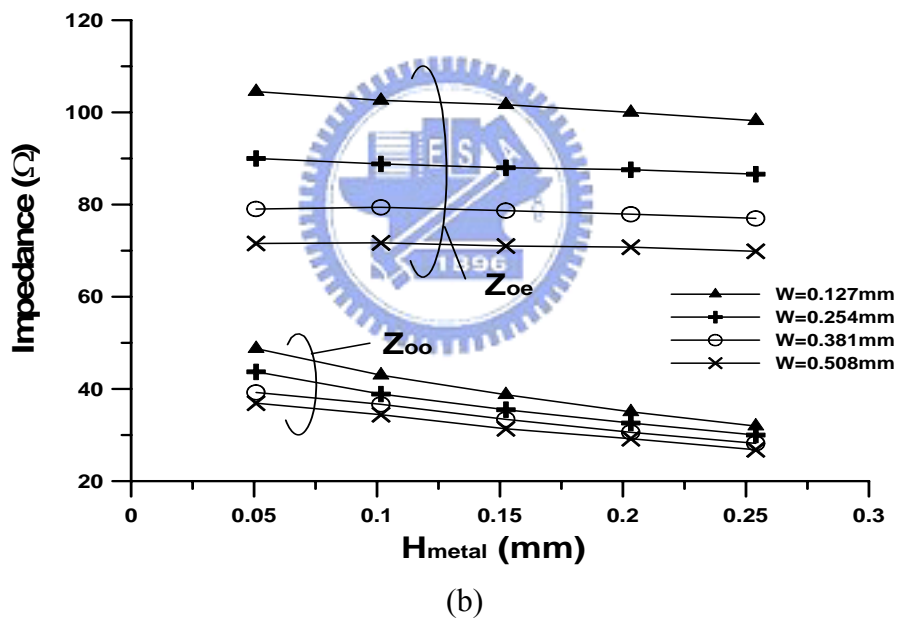
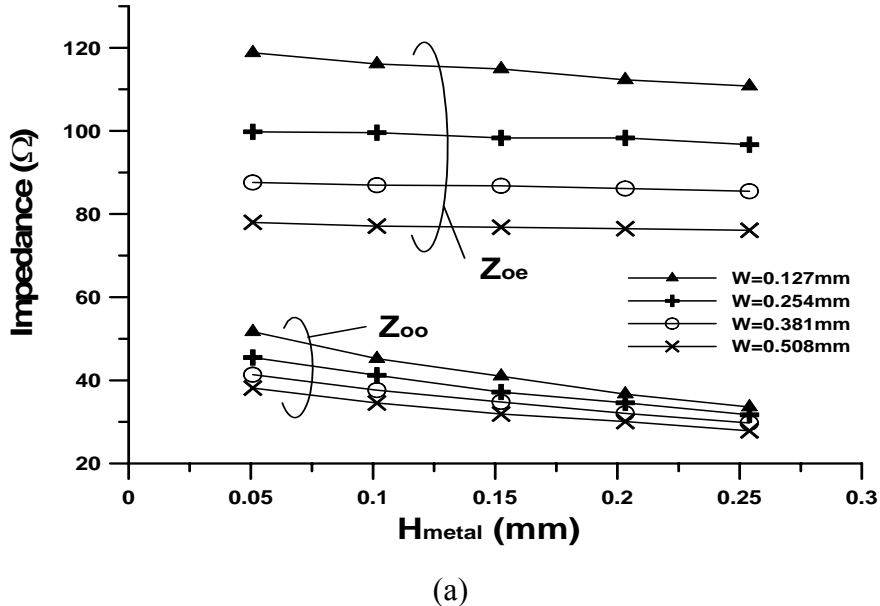


Fig. 2.2 Even- and odd-mode characteristic impedances versus VIP metal height (H_{metal}) of the type I VIP coupler with (a) $G=0.4572\text{mm}$, and (b) $G=0.7112\text{mm}$.

The type I of modified VIP coupler can not achieve coupling value as tight as -0.8dB even when W equals to 0. To implement the extremely tight-coupled center section, the type II modified VIP coupler is proposed. Fig. 2.1(b) shows the cross-sectional view of type II VIP coupler. In this Figure, the ground plane in the main substrate changes to two metal strips. Utilizing this finite-extent ground plane (in this case only two ground strips) structure, the

VIP coupler can achieve a coupling of tighter than -0.8 dB. Again, two similar dielectric blocks as those of type I structure are used to compensate the modal phase velocities. The even- and odd-mode characteristic impedances versus various VIP metal heights (H_{metal}) and ground strip spacing (G_{gnd}) are shown in Fig. 2.3(a). Similarly, G_{gnd} and H_{metal} separately control the even- and odd-mode characteristic impedances (Z_{0e} , Z_{0o}). Here the width of the ground plan strips (W_{gnd}) is chosen to be 15 mils for simplifying the design. Depicted in Fig. 2.3(b) are the even- and odd-mode effective dielectric constants versus different H_{metal} and G_{gnd} . With the help of dielectric blocks, the differences between even- and odd-mode effective dielectric constant can be minimized.

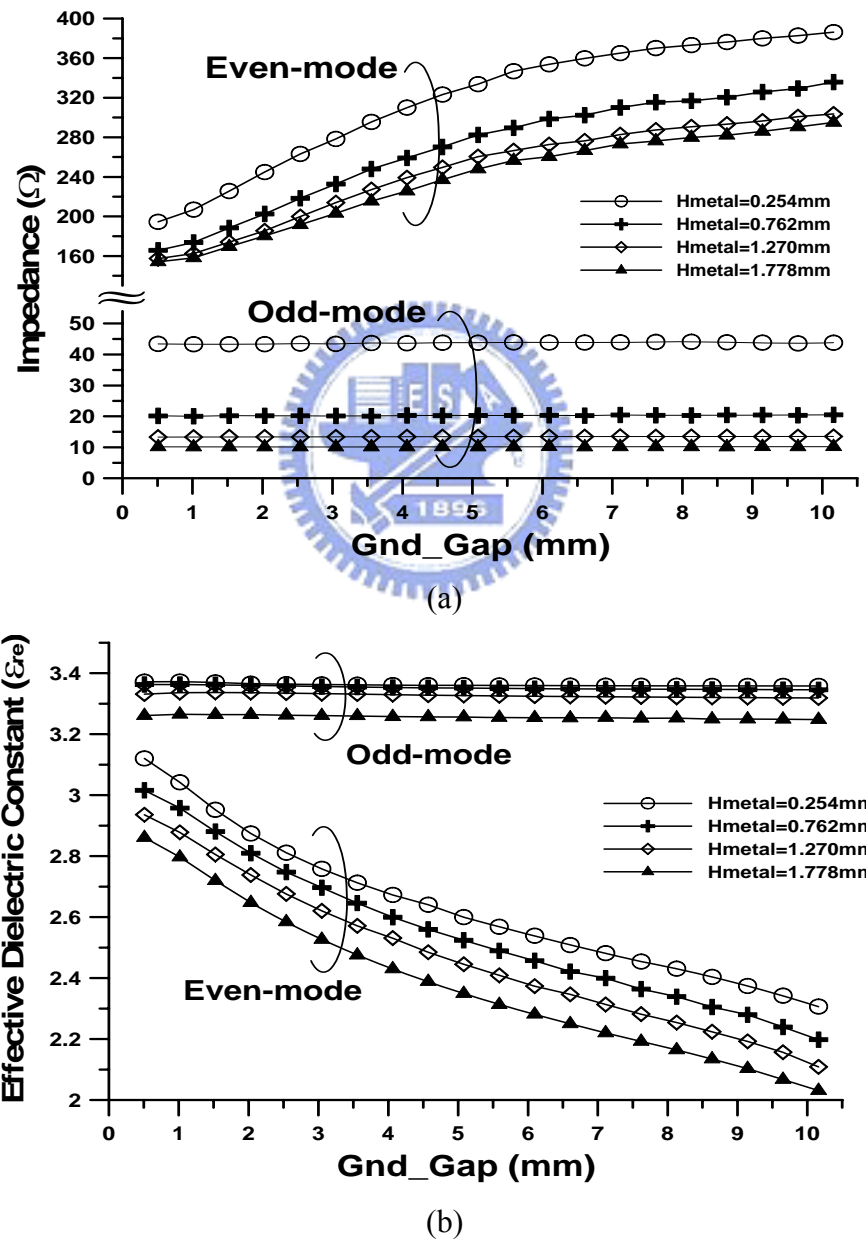


Fig. 2.3 (a) even- and odd-mode characteristic impedances, and (b) effective dielectric constants versus G_{gnd} and H_{metal} of the type II VIP coupler.

2.2 Structure of Proposed VIPSIR and SSSSIR

The proposed two filter structures are depicted in Fig. 2.4. Fig. 2.4(a) shows the structure A where the vertically installed planar stepped-impedance resonators (VIPSIRs) are adopted. In Fig. 2.4(a), the extremely tightly coupled low impedance line section is a vertically installed planar coupler while the very high impedance uncoupled-line section is also implemented on the vertical substrate. Fig. 2.4(b) depicts the structure B which uses suspended substrate stripline stepped-impedance resonators (SSSSIRs) with a similar tightly-coupled, low-impedance coupled-line section and very high impedance uncoupled-line section. For the coupled-line section, both filter structures can realize a very high even-mode impedance (Z_{0e}), and an extremely low odd-mode impedance (Z_{0o}). For the uncoupled-line section, both structures can implement a very high impedance transmission line. Although Fig. 2.4(a) and (b) show only a three-order filter, it can be extended to a filter of any order.

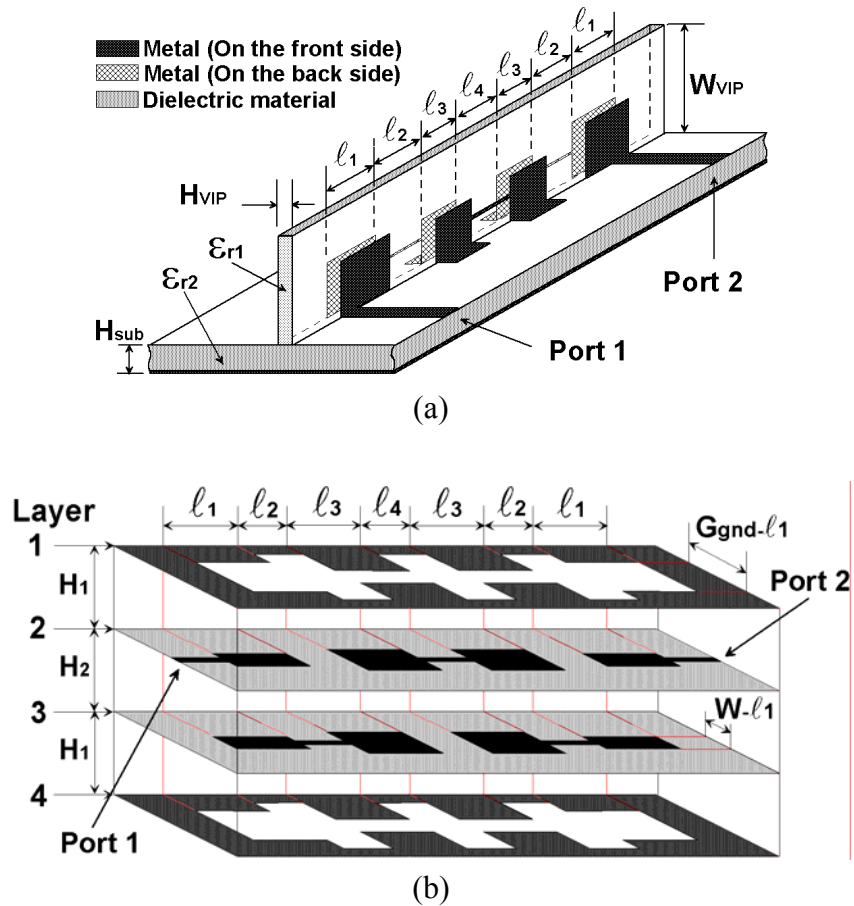


Fig. 2.4 The proposed filters structures. (a) Structure A where the vertically installed planar stepped impedance resonators are used, and (b) structure B where the modified stripline stepped impedance resonators are used.

The bandpass filter using VIP structure was first introduced by Zhao and Awai [9] where uniform impedance resonators (UIR) were used. The UIR filter causes a poor upper stopband performance. Besides, the comb-line-like filter structure in [9] is difficult to realize a filter with order higher than two due to difficulties of assembling two closely separated vertical substrates and the strong cross-coupling effects between nonadjacent vertical strips. The proposed structure A uses a single vertical substrate to implement a filter of any order and needs no backside pattern or via holes on the main substrate. Therefore, a PCB with high-density, double-sided components is allowed. Moreover, the conventional low cost, low dielectric constant substrates could be used for both vertical substrate and main substrate. Although the structure A is a three-dimensional structure and is once considered hard to implement, a properly designed soldering fixture can assemble it.

The conventional stripline or suspended stripline, which needs a complicated mechanical housing to support, is costly and difficult to assemble. Although, the cross sectional view of the proposed structure B looks somewhat like a suspended stripline structure, the proposed structure B using suspended substrate stripline with ground apertures on top and bottom plans, shows following advantage. In the suspended stripline a precisely fabricated mechanical housing is important because the even-mode impedance of the tight coupled-lines and the impedance values of high impedance lines are very sensitive to the distance between strips and the walls of the metal housing surround them. However, the fabrication and assembly tolerance of such kind of metal housing is large which leads to a poor repeatability. In contrast, the proposed filter structure B requires no metal enclosure and can be easily realized by standard low-cost multi-layer PCB fabrication process which provides almost identical result from board to board. With apertures on the top and bottom ground plane, structure B can realize a coupled line with extremely high even-mode impedance (Z_{0e}) and low odd-mode impedance (Z_{0o}) as well as an uncoupled line with very high impedance.

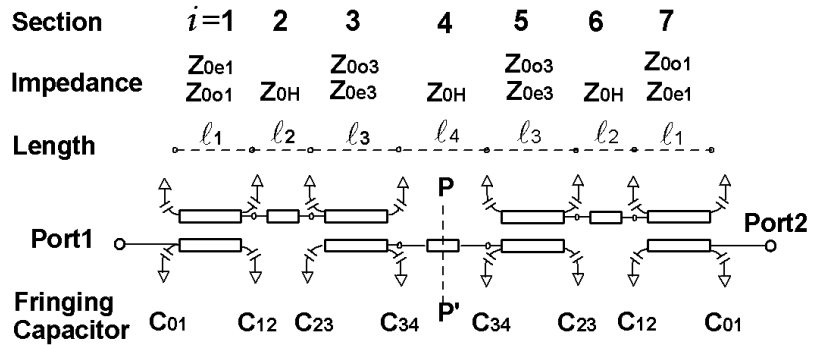


Fig. 2.5 Equivalent circuit for structure A and B in Fig. 2.4, where P-P' is the symmetrical plane.

The equivalent circuit of the proposed filter using structure A or B is shown in Fig. 2.5. The circuit parameters in the equivalent circuit will be extracted and be transformed into a series of design charts corresponding to structure A and B, respectively. Therefore, the proposed filters can be designed by a circuit simulator with good accuracy following these design charts without using of time consuming EM simulator. In chapter 4, the proposed design procedures have been examined with several examples where the measured results confirm very well with the simulated ones.

2.3 Analysis and Characteristic of Proposed Filter Structure

2.3.1 Characteristics of Filter structure A

Fig. 2.4(a) illustrates the configuration of proposed filter structure A where a main substrate and a vertical substrate are installed as shown. The stepped impedance resonators (SIRs) are patterned on the front and backside of the vertical substrate in a parallel-coupled manner such that the equivalent circuit in Fig. 2.5 could characterize the filter. In Fig. 2.5, the coupled-line sections represent the vertically installed planar (VIP) coupled lines; the uncoupled transmission lines represent the high impedance lines on the vertical substrate, and the capacitors represent the open-end and step-junction fringing capacitance. Each of them is discussed in detail as following.

First, the cross-sectional physical parameters of a VIP coupled line and a high impedance line are shown in Fig. 2.6(a) and (b), respectively. The parameters used in the design charts are similar to Fig. 2.6 unless otherwise specified in each figure. In order to characterize the properties of the coupled-line section of filter structure A, a 3D EM simulator, HFSS, is applied to extract the even- and odd-mode characteristic impedances (Z_{0e} , Z_{0o}) and the corresponding effective dielectric constants (ϵ_{ree} , ϵ_{reo}). Fig. 2.7 depicts the modal characteristic impedances versus the strip width (W_{LZ}) on the vertical substrate with various patch widths (W) on the main substrate. The corresponding modal effective dielectric constants (ϵ_{ree} , ϵ_{reo}) are shown in Fig. 2.8. The modal characteristic impedances varying with respect to W and W_{LZ} can be summarized as follows. Increasing the patch width (W) on the main substrate would mainly decrease the even-mode impedance and increasing the strip width (W_{LZ}) on the vertical substrate would mainly decrease the odd-mode impedance. The even-mode effective dielectric constant decreases as the patch width (W) and the strip width (W_{LZ}) reduce. On the other hand, the odd-mode effective dielectric constants approach to a constant as increasing the strip width (W_{LZ}). With the help of the design curves in Figs. 2.7 and 2.8, the physical dimensions of a vertically installed planar-coupled line corresponding to a specified Z_{0e} and Z_{0o} could be obtained easily.

Second, the high-impedance, uncoupled line on the vertical substrate as shown in Fig.

2.6(b) leads to a high impedance ratio ($R=Z_{0H} / Z_{0L}$) of a stepped impedance resonator (SIR). Higher impedance of the uncoupled line implies broader upper stopband clearance of the filter structure A. The characteristic of uncoupled line on the vertical substrate is depicted in Fig. 2.9, which shows the characteristic impedances and effective dielectric constants of the high impedance line versus distance (D_{HZ}) between high-impedance line and the main substrate. It is clear that increasing the distance (D_{HZ}) would increase the characteristic impedance of the high impedance line. Although decreasing the metal width (W_{HZ}) of the high impedance line will also slightly affect the line impedance, it is not the main factor to control the line impedance. Therefore, the line width (W_{HZ}) is fixed to be 0.254mm (10mils) in our design in order to tradeoff between higher characteristic impedance and good PCB etching accuracy.

Last, the open-end and step-junction fringing capacitance increase according to the strip width (W_{LZ}) on the vertical substrate. The accurate capacitance value can be extracted from EM simulated results. As a result, the capacitance approaches to a limiting value of 0.03pF as the strip width (W_{LZ}) on the vertical substrate greater than 0.762mm (30mils). Fortunately, the strip width (W_{LZ}) on the vertical substrate is always greater than 0.762mm (30mils) in our filter examples so that the fringe capacitance could be set as 0.03pF.

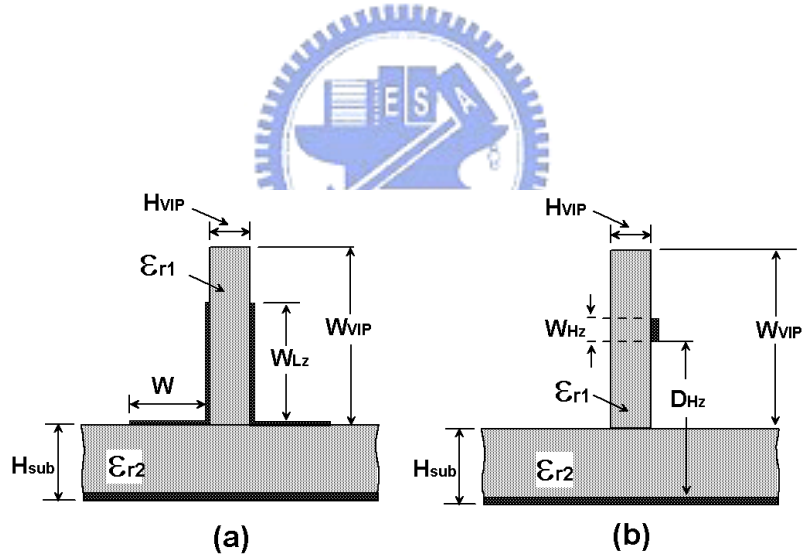
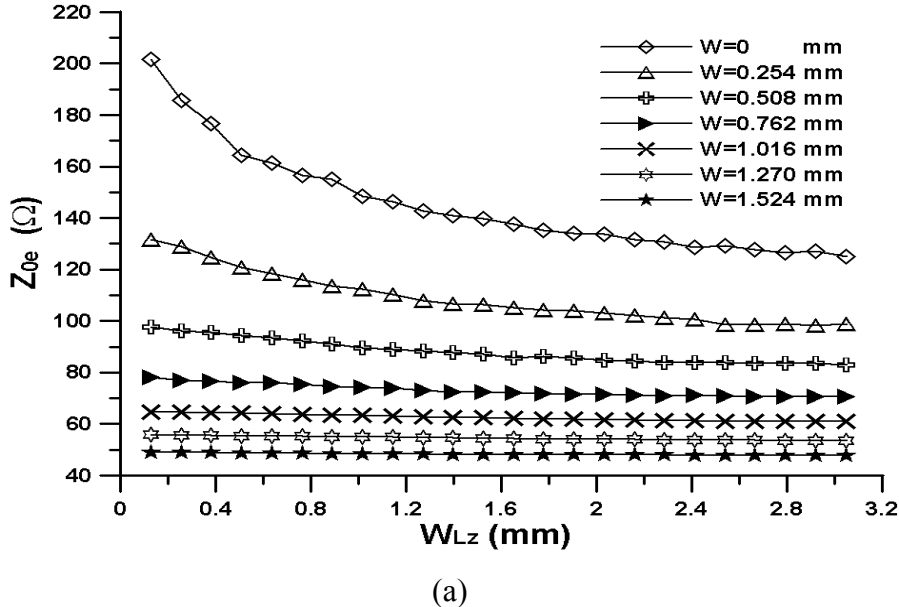
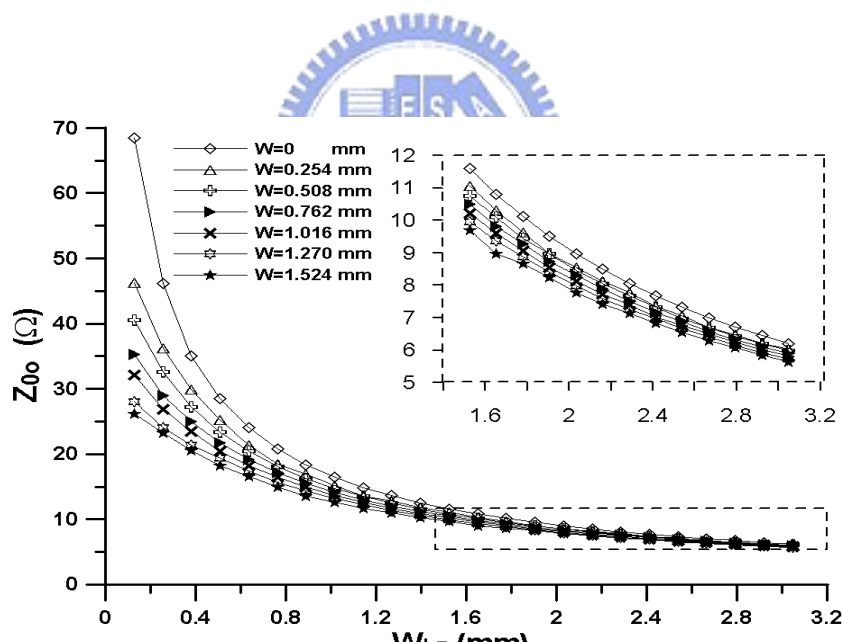


Fig. 2.6 Cross-sectional views of filter structure A. (a) vertically installed planar-coupled line, and (b) high impedance uncoupled line, where $H_{sub}=0.508\text{mm}$, $H_{VIP}=0.2032\text{mm}$, $W_{HZ}=0.254\text{mm}$, $W_{VIP}=3.048\text{mm}$, and $\epsilon_{r1}=\epsilon_{r2}=3.38$ are chosen in this paper.

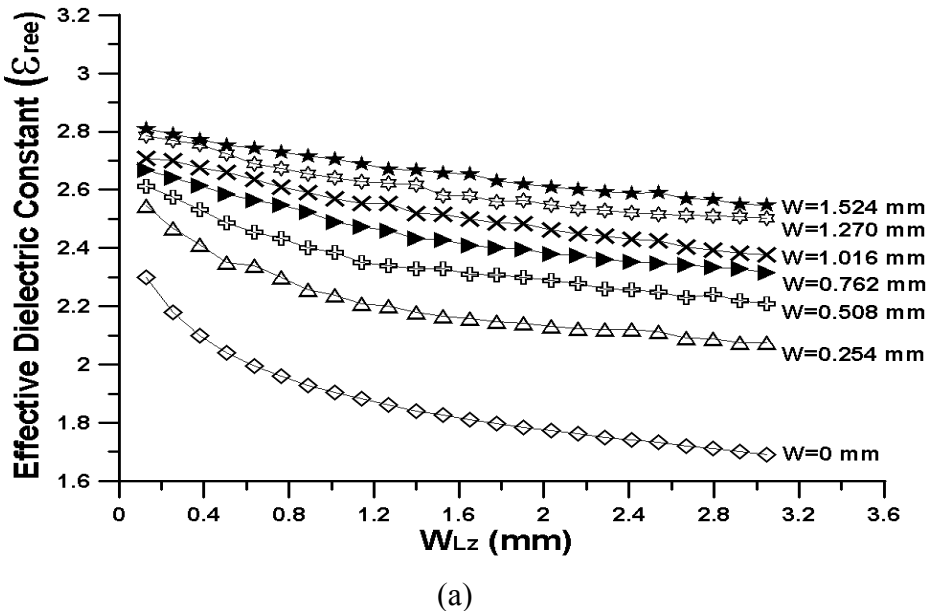


(a)

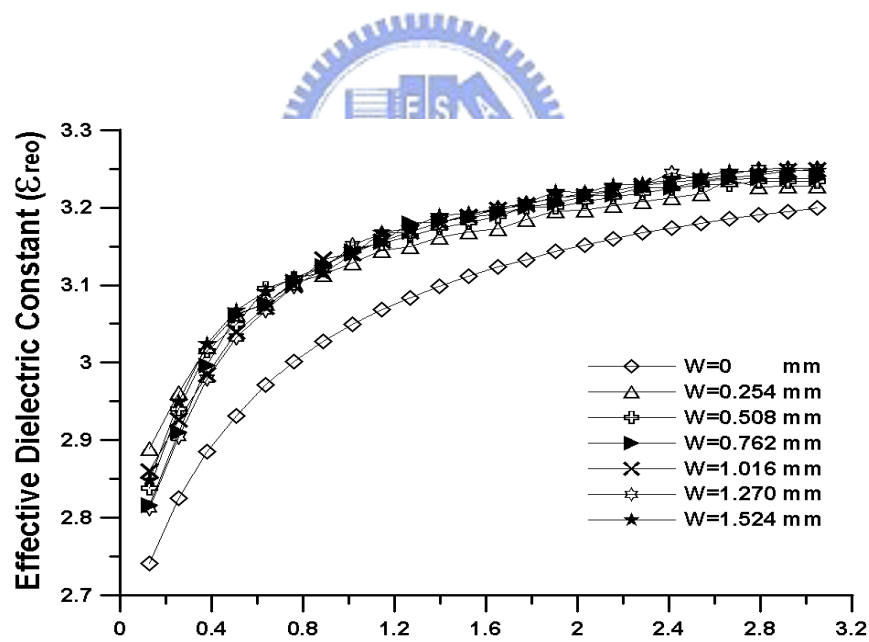


(b)

Fig. 2.7 (a) Even-mode and (b) Odd-mode characteristic impedances versus strip width (W_{Lz}) on the vertical substrate with various patch width (W) on the main substrate, where $H_{sub}=0.508\text{mm}$, $H_{VIP}=0.2032\text{mm}$, $W_{HZ}=0.254\text{mm}$, $W_{VIP}=3.048\text{mm}$, and $\epsilon_{r1}=\epsilon_{r2}=3.38$.



(a)



(b)

Fig. 2.8 (a) Even-mode and (b) Odd-mode effective dielectric constants versus strip width (W_{Lz}) on the vertical substrate with various patch width (W) on the main substrate, where $H_{sub}=0.508\text{mm}$, $H_{VIP}=0.2032\text{mm}$, $W_{HZ}=0.254\text{mm}$, $W_{VIP}=3.048\text{mm}$, and $\epsilon_{rl}=\epsilon_{r2}=3.38$.

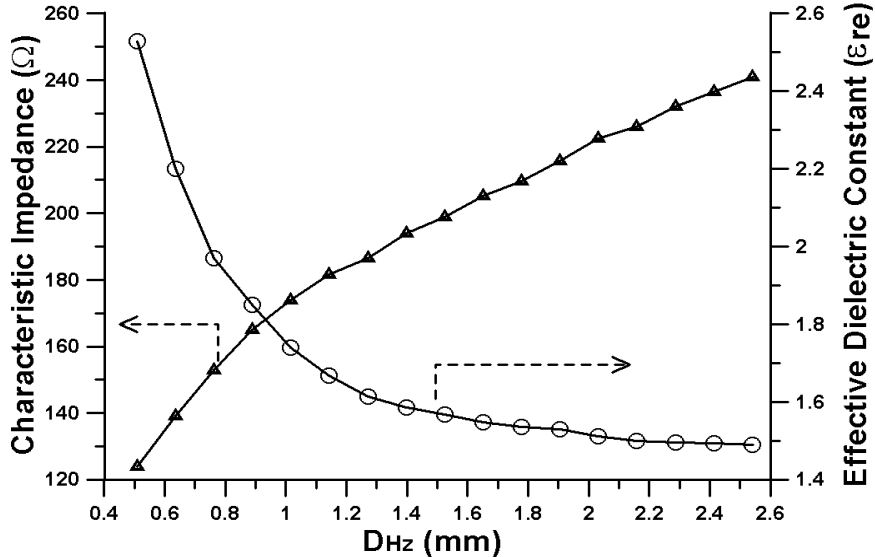
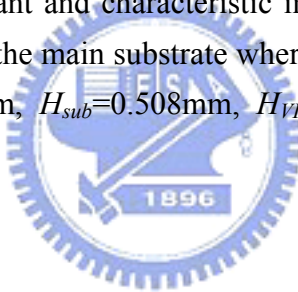


Fig. 2.9 Effective dielectric constant and characteristic impedance versus the distance (D_{HZ}) between high impedance line and the main substrate where the strip width W_{HZ} on the vertical substrate is fixed to be 0.254mm, $H_{sub}=0.508$ mm, $H_{VIP}=0.2032$ mm, $W_{VIP}=3.048$ mm, and $\epsilon_{r1}=\epsilon_{r2}=3.38$.



2.3.2 Characteristics of Filter Structure B

The proposed filter structure B is realized by the conventional multi-layer PCB fabrication process. There are totally four layers of conductor. The top (first) and bottom (fourth) layers are ground conductors and the second and third layers are the broadside-coupled, stepped impedance resonators. The broadside-coupled lines form the strong coupling sections and high impedance uncoupled lines provide the high impedance ratio of the SIR. Therefore, the same equivalent circuit as shown in Fig. 2.10 could also be applied to the filter structure B. The cross sectional view of broadside-coupled line and the high impedance uncoupled line are depicted in Fig. 2.10(a) and (b), respectively. Structure B has the benefit of easy fabrication. However, comparing to structure A, structure B can not use its aperture region of both upper and bottom side of the substrate to place circuit components. Using the EM simulator, HFSS, the similar design curves of Z_{0e} , Z_{0o} and ϵ_{ree} , ϵ_{re0} corresponding to various ground aperture size (G_{gnd}) and coupled-line widths (W) can be extracted as shown in Fig. 2.11-2.12. Due to the odd-mode EM field being bounded within the coupling strip, the Z_{0o} is mainly controlled by W and is almost independent of the value of

G_{gnd} . On the other hand, if G_{gnd} is greater than W , the Z_{0e} increases as the G_{gnd} increases. These characteristics make it simple to obtain the required values of Z_{0e}/Z_{0o} by only adjusting W and G_{gnd} . Fig. 2.13 illustrates the effective dielectric constant and characteristic impedance of the high impedance line as a function of ground aperture size (G_{gnd}). Here, the line width W_{HZ} is fixed to be 0.2032mm (8 mils) in our design in order to tradeoff between higher characteristic impedance and good PCB etching accuracy.

The values of fringing capacitors of structure B are larger and more complicated than structure A. Therefore, effort should be paid to extract their values more accurately. The extraction of fringing capacitance values can be done easily by computer optimization where the fringing capacitors correlate the scattering parameters of the circuit model and the results from EM simulation. In our proposed filter structure B, the step-junction capacitance could be considered to be the same as the open-end capacitance due to the large abrupt change on the junction width. The fringing capacitors of each section could be extracted separately, thus, the efforts of EM simulation and circuit extraction could be reduced.

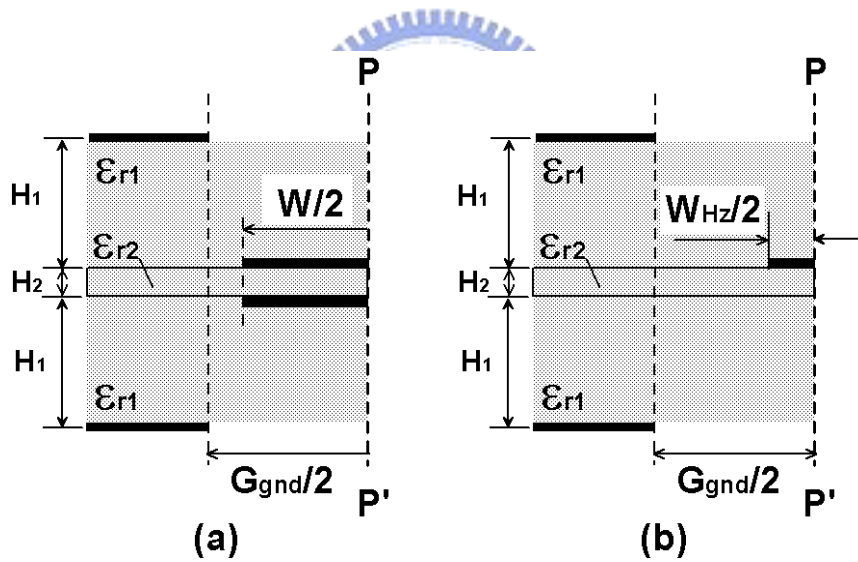


Fig. 2.10 Cross-sectional views of the filter structure B. (a) broadside-coupled line, and (b) high impedance uncoupled line, where $H_1=0.508\text{mm}$, $H_2=0.2032\text{mm}$, $W_{HZ}=0.2032\text{mm}$, $\epsilon_{r1}=\epsilon_{r2}=3.38$, and P-P' is the symmetrical plane. Due to symmetry only half of the structures are shown.

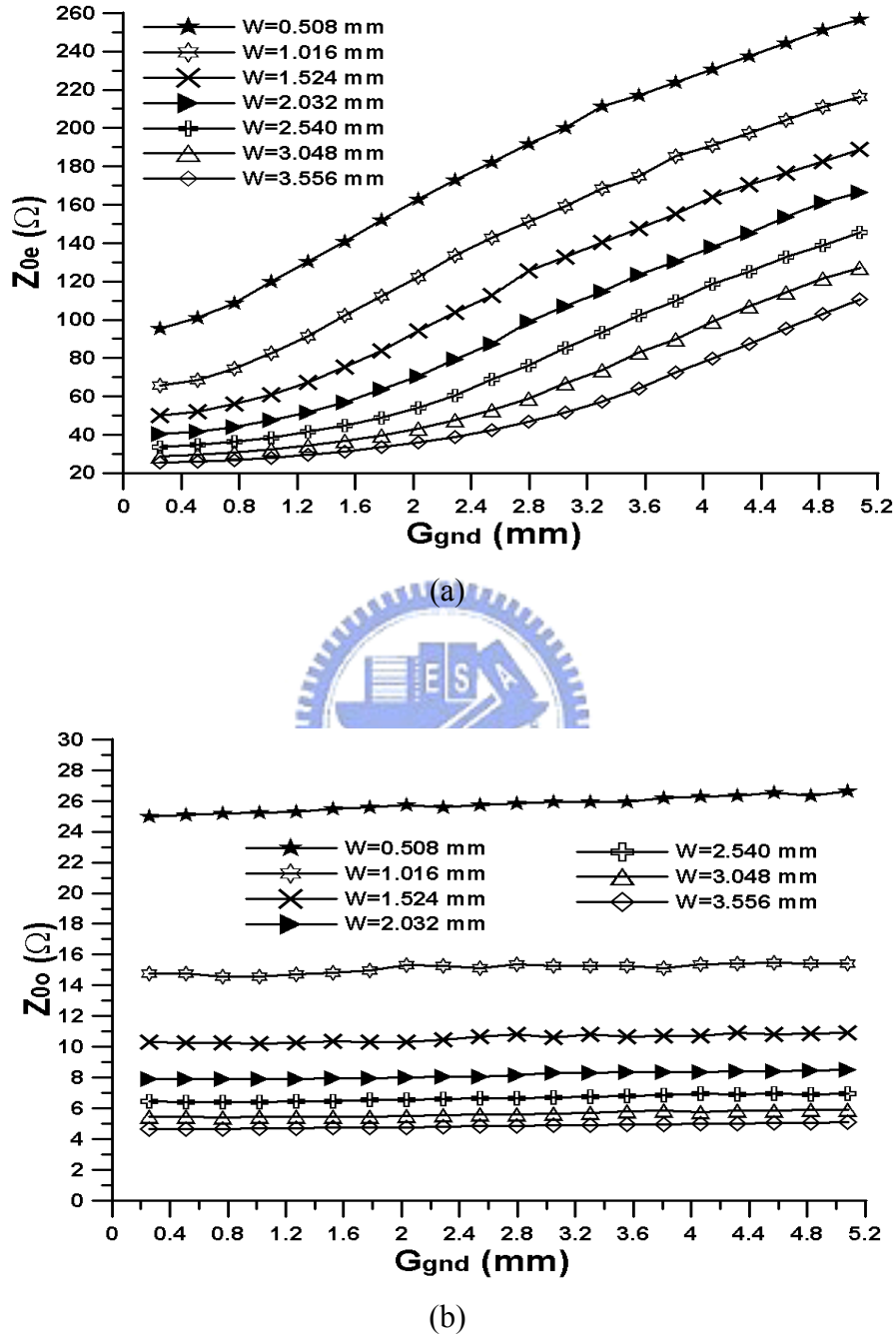
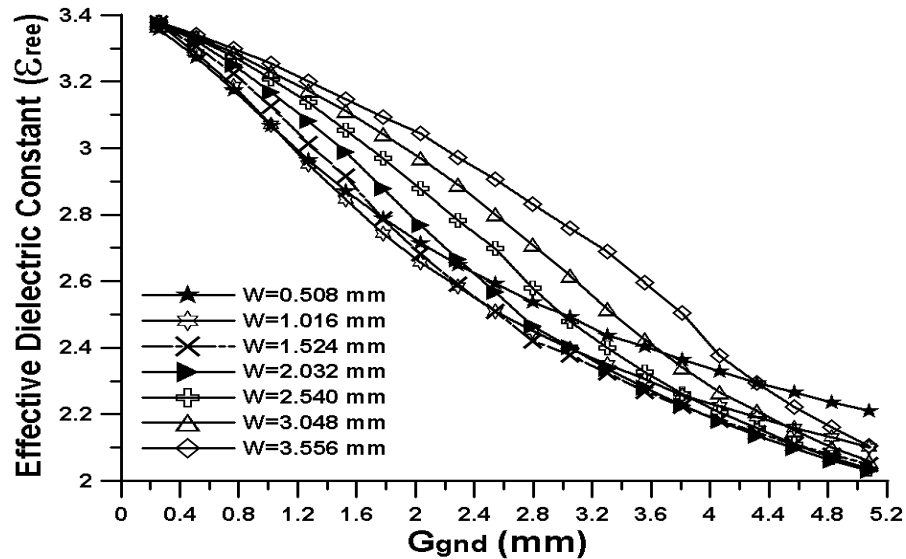
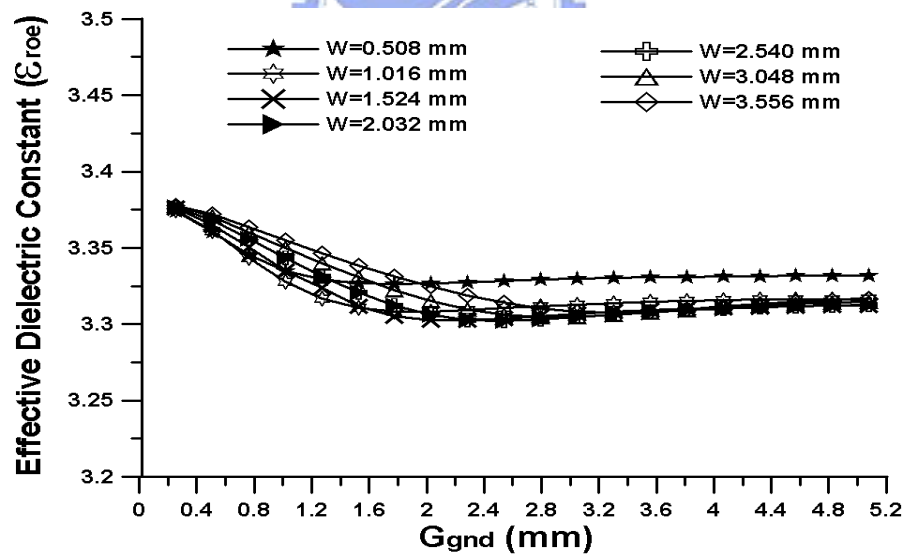


Fig. 2.11 (a) Even-mode and (b) Odd-mode characteristic impedances versus ground plane aperture size (G_{gnd}) with various broadside coupled-line width (W), where $H_1=0.508\text{mm}$, $H_2=0.2032\text{mm}$, $W_{HZ}=0.2032\text{mm}$, and $\epsilon_{r1}=\epsilon_{r2}=3.38$.



(a)



(b)

Fig. 2.12 (a) Even-mode and (b) Odd-mode effective dielectric constants versus ground plane aperture size (G_{gnd}) with various broadside coupled-line widths (W), where $H_1=0.508\text{mm}$, $H_2=0.2032\text{mm}$, $W_{HZ}=0.2032\text{mm}$, and $\epsilon_{r1}=\epsilon_{r2}=3.38$.

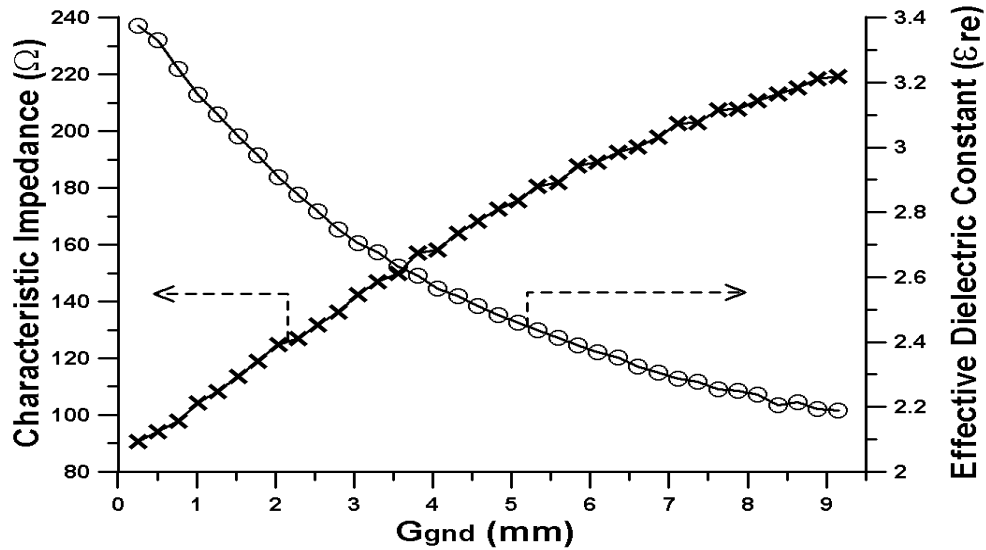


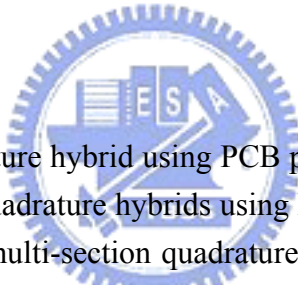
Fig. 2.13 Effective dielectric constant and characteristic impedance of uncoupled line versus the ground plane aperture size (G_{gnd}), where $H_1=0.508\text{mm}$, $H_2=0.2032\text{mm}$, $W_{HZ}=0.2032\text{mm}$, and $\epsilon_{r1}=\epsilon_{r2}=3.38$.



Chapter 3

Analysis, Design and Realization of Ultra-Broadband Multi-Section Quadrature Hybrid

3.1 Literature Survey



A single-section VIP quadrature hybrid using PCB process has been demonstrated in [6, 7] but none of the multi-section quadrature hybrids using PCB process has been reported. The most difficult issues to realize a multi-section quadrature hybrid are achieving the extremely tight-coupled center section, equalizing the modal phase velocities, and minimizing the discontinuity effect between each section. In the past, only strip line circuit can solve all these three problems. Unfortunately, unlike microstrip circuit, the stripline circuit needs a complex metal housing. For microstrip implementation, Lange [3] coupler using high dielectric constant substrate can achieve tight coupling of about -3dB but it is not suitable for PCB process (due to PCB's low dielectric constant substrate) and could not achieve required -0.8dB of coupling. Besides, multi-section quadrature hybrid using Lange coupler and parallel-coupled lines encounters serious discontinuity problem at the junction between each section. VIP coupler in [7] solves the problem of PCB realization of tight coupled lines but their modal phase velocities are not compensated. And according to our analysis, the structure in [7] can not realize a coupler with coupling as tight as -0.8dB. Many studies [10-14] have been conducted to compensate the modal phase velocities of a coupler. However, none of them is suitable for VIP coupler. In this chapter, we adopt two modified VIP couplers as discussed in chapter 1 to overcome the realization challenges of a 5-section ultra-broadband quadrature hybrid. The two outer sections use conventional microstrip parallel-coupled lines and the three inner sections comprise two types of modified VIP couplers where one of them provides extra layout flexibility for minimizing the discontinuity between each section.

Moreover, special dielectric blocks are proposed to equalize the modal phase velocities of the proposed modified VIP couplers which have been discussed in chapter 2.

3.2 Theory and Design Procedures

The schematic circuit representation of a single-section coupler is shown in Fig. 3.1 where the port 1 is the input port, port 2 is the through port, port 3 is the coupled port and port 4 is the isolated port. Because the network is symmetrical about the plan P-P', the even- and odd-mode analysis could be adopted. The 4-ports network shown in Fig. 3.1 could be analyzed easily by decomposed into even- and odd-mode excitation as shown in Fig. 3.2(a) and (b), respectively. In Fig. 3.2(a) and (b), the Z_{0e} and Z_{0o} are the characteristic impedances and θ_e and θ_o are the transmission phases of the even and odd mode, respectively.

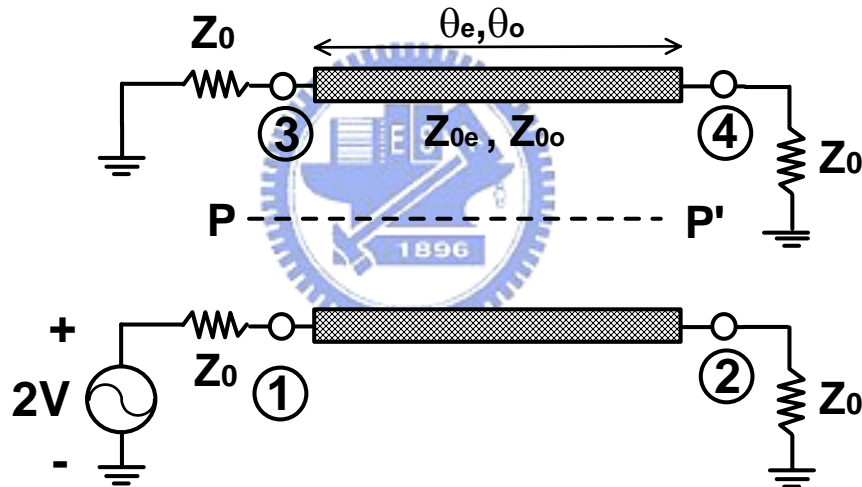
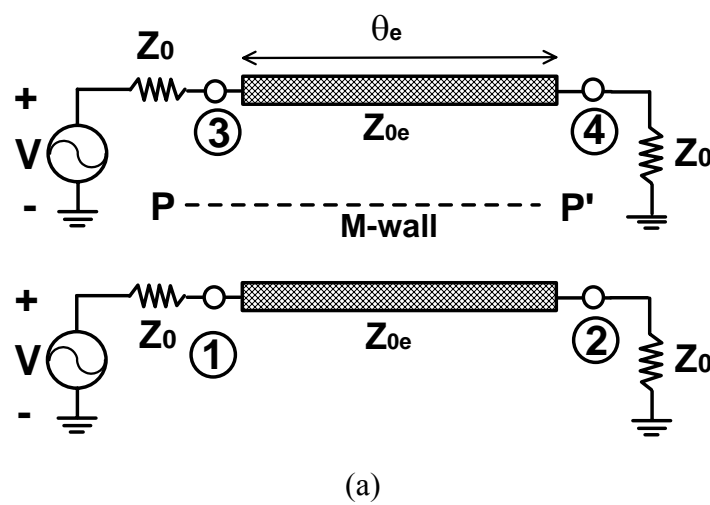


Fig. 3.1 Schematic circuit representation of a single-section coupler.



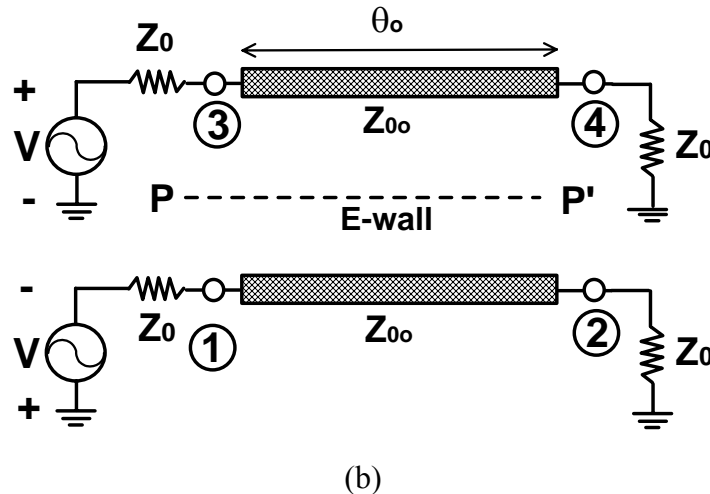


Fig. 3.2 Schematic circuit expression of coupler with (a) even mode excitation and (b) odd mode excitation.

Using these equivalent circuits, the ABCD matrices of the even- and odd-mode excitation can be expressed as

$$\begin{bmatrix} A_e & B_e \\ C_e & D_e \end{bmatrix} = \begin{bmatrix} \cos \theta_e & jZ_{0e} \sin \theta_e \\ jY_{0e} \sin \theta_e & \cos \theta_e \end{bmatrix} \quad (3.1)$$

And

$$\begin{bmatrix} A_o & B_o \\ C_o & D_o \end{bmatrix} = \begin{bmatrix} \cos \theta_o & jZ_{0o} \sin \theta_o \\ jY_{0o} \sin \theta_o & \cos \theta_o \end{bmatrix} \quad (3.2)$$

And, the corresponding even- and odd-mode scattering matrices can be obtained.

$$[S_e] = \begin{bmatrix} S_{11e} & S_{21e} \\ S_{21e} & S_{22e} \end{bmatrix} \quad (3.3)$$

$$[S_o] = \begin{bmatrix} S_{11o} & S_{21o} \\ S_{21o} & S_{22o} \end{bmatrix} \quad (3.4)$$

Where,

$$S_{11e} = S_{22e} = \frac{j\left(\frac{Z_{0e}}{Z_0} - \frac{Z_0}{Z_{0e}}\right) \sin \theta_e}{2 \cos \theta_e + j\left(\frac{Z_{0e}}{Z_0} + \frac{Z_0}{Z_{0e}}\right) \sin \theta_e} \quad (3.5)$$

$$S_{11o} = S_{22o} = \frac{j\left(\frac{Z_{0o}}{Z_0} - \frac{Z_0}{Z_{0o}}\right) \sin \theta_o}{2 \cos \theta_o + j\left(\frac{Z_{0o}}{Z_0} + \frac{Z_0}{Z_{0o}}\right) \sin \theta_o} \quad (3.6)$$

$$S_{21e} = \frac{2}{2\cos\theta_e + j(\frac{Z_{0e}}{Z_0} + \frac{Z_0}{Z_{0e}})\sin\theta_e} \quad (3.7)$$

$$S_{21o} = \frac{2}{2\cos\theta_o + j(\frac{Z_{0o}}{Z_0} + \frac{Z_0}{Z_{0o}})\sin\theta_o} \quad (3.8)$$

and Z_0 is the port impedance of the coupler.

Finally, after composition of these modal parameters, the various elements in the 4-port scattering matrix are given as follows:

$$\begin{aligned} S_{11} &= \frac{S_{11e} + S_{11o}}{2}, S_{12} = S_{21}, S_{13} = S_{31}, S_{14} = S_{41} \\ S_{21} &= \frac{S_{21e} + S_{21o}}{2}, S_{22} = \frac{S_{22e} + S_{22o}}{2}, S_{23} = S_{41} \\ S_{24} &= \frac{S_{22e} - S_{22o}}{2}, S_{31} = \frac{S_{11e} - S_{11o}}{2}, S_{32} = S_{41}, S_{33} = S_{11}, S_{34} = S_{21} \\ S_{41} &= \frac{S_{21e} - S_{21o}}{2}, S_{42} = S_{24}, S_{43} = S_{21}, S_{44} = S_{22} \end{aligned} \quad (3.9)$$

Following conditions should be satisfied for perfect port match and isolation.

$$S_{11e} = -S_{11o}, S_{22e} = -S_{22o}, \text{ and } S_{21e} = S_{21o}$$

Comparing (3.5) and (3.6), the conditions $S_{11e} = -S_{11o}$ and $S_{22e} = -S_{22o}$ are satisfied for arbitrary transmission phase θ (assuming $\theta = \theta_e = \theta_o$) as long as

$$\frac{Z_{0e}}{Z_0} = \frac{Z_0}{Z_{0o}}$$

or

$$Z_{0e}Z_{0o} = Z_0^2 \quad (3.10)$$

The equation (3.10) is also satisfied the condition ($S_{21e} = S_{21o}$) under the condition $\theta = \theta_e = \theta_o$. Therefore, (3.10) gives the necessary condition for TEM backward-wave directional coupler. When the propagation wave is non TEM wave ($\theta_e \neq \theta_o$), only $Z_{0e} = Z_{0o}$ can satisfied the matching condition at all ports. However, there is no meaning for a coupler to set $Z_{0e} = Z_{0o}$. In other words, theoretically, only TEM mode propagation structure can realize a matched coupler. However, in practical application for a single-section coupler even the phase different between even- and odd-mode is over 30% the return loss is still in acceptable value of 15dB.

From (3.9) and (3.10) assuming ($\theta = \theta_e = \theta_o$), we obtain

$$S_{21} = \frac{Z_0}{2Z_0 \cos\theta + j(Z_{0e} + Z_{0o})\sin\theta} \quad (3.11)$$

$$S_{31} = \frac{(Z_{0e} - Z_{0o})}{(Z_{0e} + Z_{0o}) - j2\sqrt{Z_{0e}Z_{0o}} \cot\theta} \quad (3.12)$$

From equation (3.11) and (3.12) we know that the coupling (S_{31}) and the through (S_{21}) of the coupler are both a function of θ . And when the $\theta = \frac{\pi}{2}$, the coupling could be simplified as

$$K = \frac{Z_{0e} - Z_{0o}}{Z_{0e} + Z_{0o}} \quad (3.13)$$

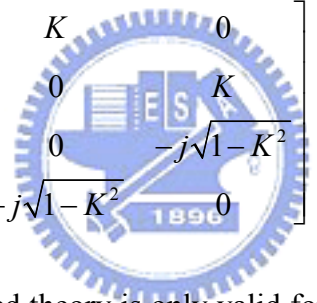
In equation (3.13) K is called the coupling factor which defines as the coupling at the central frequency of a coupler. Therefore, the maximal coupling between port 1 and 3 (or port 2 and 4) occurs when $\theta = \frac{\pi}{2}$ and the maximal coupling values are given by

$$|S_{31}| = |S_{13}| = |S_{24}| = |S_{42}| = K$$

Further, when $\theta = \frac{\pi}{2}$

$$|S_{21}| = |S_{12}| = |S_{34}| = |S_{43}| = \sqrt{1 - K}$$

Thus, the scattering matrix of a backward-wave coupler with quarter-wave length can be represented as follows:

$$[S] = \begin{bmatrix} 0 & -j\sqrt{1-K^2} & K & 0 \\ -j\sqrt{1-K^2} & 0 & 0 & K \\ K & 0 & 0 & -j\sqrt{1-K^2} \\ 0 & K & -j\sqrt{1-K^2} & 0 \end{bmatrix} \quad (3.14)$$


Although the above described theory is only valid for a single-section direction coupler, it is the basic building block of a multi-section directional coupler. Each section of multi-section directional coupler is a single-section direction coupler with designed coupling factor so that a good single-section directional coupler is the most important part to build a multi-section directional coupler.

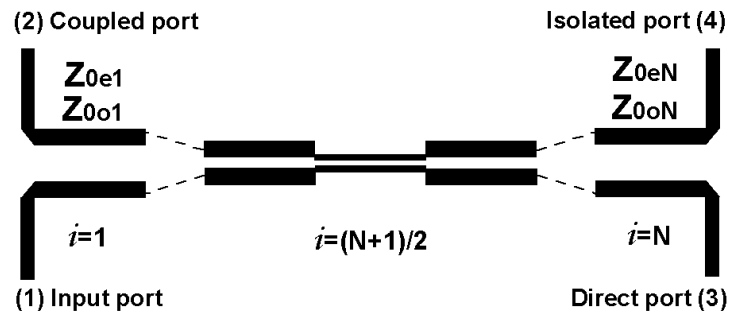


Fig. 3.3 A N-section cascaded symmetrical quadrature hybrid.

In order to obtain a near-constant coupling over a wider frequency range, a multi-section coupler structure is the most commonly used method. The multi-section coupler cascades several sections of coupler with various coupling factors. Each section is quarter wave length long at center frequency. By properly choosing the even- and odd-mode impedances of each section, the multi-section coupler could have a Chebyshev or Butterworth type of response over a broad bandwidth. The multi-section coupler could be either symmetrical or asymmetrical. Shown in Fig. 3.3 is a symmetrical multi-section coupler. For a 90^0 quadrature coupler, the circuit should be symmetric. An N-section directional coupler contains N different single-section coupler in a cascaded manner. Each single section is denoted by the even- and odd-mode characteristic impedances. As shown in Fig.2.2b, the i-th section in symmetrical coupler will be identical to the $(N+1-i)$ th section. The signal goes out from the through port is 90^0 out of phase to that of the coupled port ($\angle S_{31} = \angle S_{21} + 90$ degree). This phase relationship is independent of frequency. Because of this property, the 3-dB symmetrical directional couplers are widely used in several microwave circuits such balanced amplifier, balanced mixer, phase shifter, power divider, and beam-forming network for array antennas and for direction-finding antennas. The asymmetrical multi-section coupler does not have the mentioned phase property as symmetrical one and is not as popular as symmetrical multi-section coupler. Here, only the symmetrical multi-section coupler will be discussed.

An analytical design expression of a multi-section directional coupler is very cumbersome even the order is small. However, synthesis of multi-section symmetrical TEM coupler using insertion loss method has been presented by Cristal and Young [15]. Moreover, the design tables for equal-ripple and maximally flat responses of multi-section symmetrical coupler up to nine sections are generated in [15]. Therefore, the design procedures of multi-section cascaded coupler are described as follow.

- 1) According to the specification for desired coupler, utilize the design table to obtain the required number of sections and the even- and odd-mode characteristic impedances of each section. Here, a 5-section symmetrical 3dB quadrature hybrid is chosen as an example.
- 2) Usually, the outmost sections (section 1 and 5) are the most loosely coupled sections. The conventional parallel-coupled microstrip lines are suitable for these sections. For this kind of coupled lines, commercial circuit simulators such as ADS, or Microwave Office can get the physical dimensions easily.
- 3) Use Fig. 2.3 (a) and (b) to obtain the physical dimensions of the central section (section 3) which is the most critical one.
- 4) Last, to design the inner sections (section 2 and 4), designers should properly choose the width and distance of the strips on the main substrate by the aid of Fig. 2.2 (a) and (b) to minimize the discontinuities between sections (especially between the outmost sections).

5) Finally, the whole multi-section quadrature hybrid performances are verified by 3-D EM simulator HFSS.

3.3 Ultra-Broadband Multi-Section Quadrature Hybrid Using Modified VIP Coupler

In this section, a quadrature hybrid with a passband ripple of +/- 0.5dB and frequency range of 1-9GHz is demonstrated. According to the design table listed in [9], five sections are needed to fulfill such specifications and the corresponding even- and odd-mode characteristic impedances of each section are detailed in table 3.1.

Table 3.1 Design parameters and physical dimensions of experimental coupler

Coupler Specifications						Dimension (mm)				
Freq	C (dB)	Ripple	Section	Z_{0e}	Z_{0o}	W	G	H_{metal}	G_{gnd}	L
1-9GHz	3dB	+/-0.5dB	I=1,5	58.8	42.5	1.1	0.38	NA	NA	9.0
			I=2,4	78.5	31.8	0.4	0.6	0.16	NA	8.0
			I=3	233	10.7	NA	NA	1.5	6.6	8.5

Based on the above design procedures, the proposed 5-section hybrid is fabricated. The detail physical dimensions of each section are also shown in Table 3.1. The photograph of the proposed 5-section hybrid is shown in Fig. 3.4. The main substrate, VIP substrate and dielectric blocks are all Rogers RO4003 with dielectric constant of 3.38 and thickness of 0.508mm (20mils), 0.2032mm (8mils) and 1.524mm (60 mils) respectively.

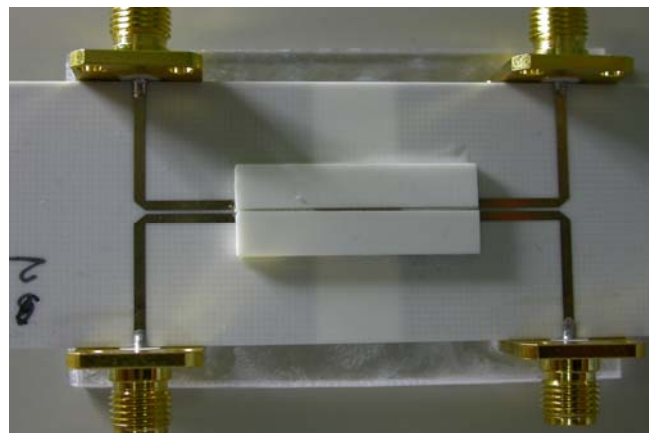


Fig. 3.4 Photograph of the fabricated five-section 3dB directional coupler.

Depicted in Fig. 3.5 and 3.6 are the simulated and the measured results that a perfect match could be observed. The simulated and measured amplitude and phase errors are shown in Fig. 3.7. The measured amplitude and phase balances between port 2 (coupled port) and port 3 (through port) are described as following. The amplitude imbalance is less than $+-0.65\text{dB}$ and phase difference is keeping within $90^\circ +/ - 5^\circ$ over the designed frequency of 1-9GHz.

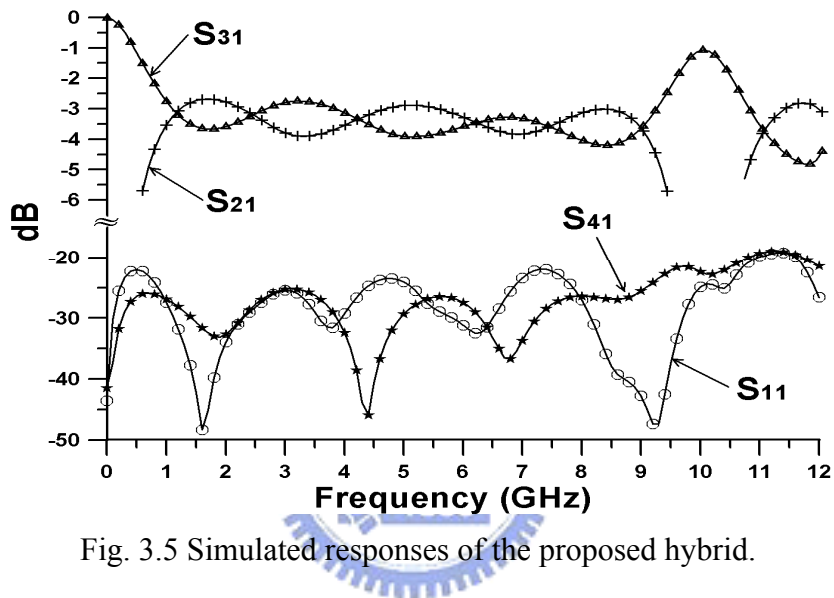


Fig. 3.5 Simulated responses of the proposed hybrid.

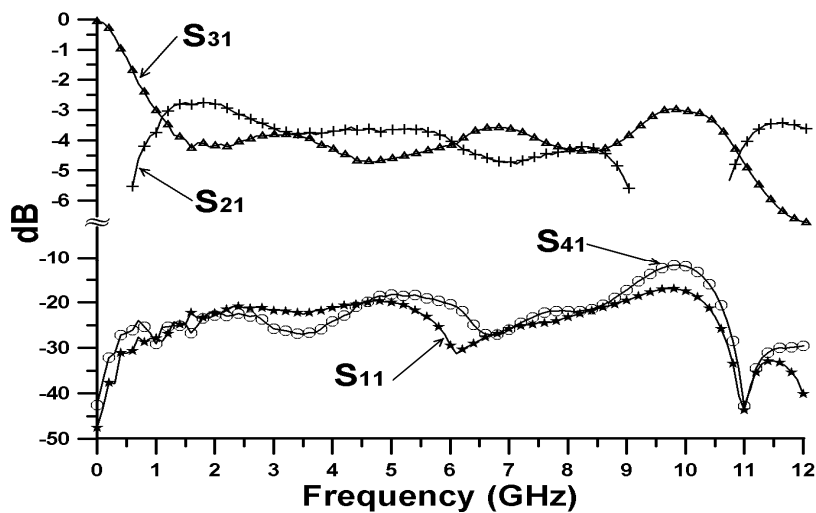


Fig. 3.6 Measured responses of the proposed hybrid.

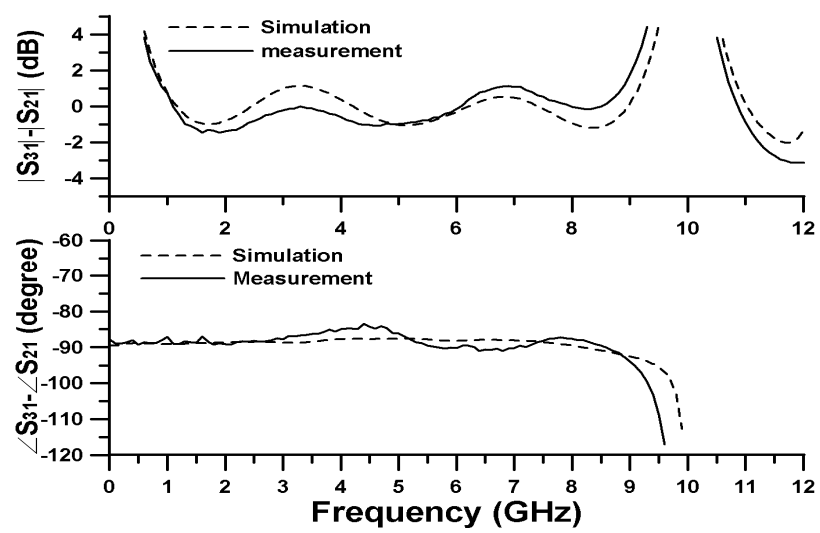


Fig. 3.7 Measured and simulate amplitude and phase errors of the proposed hybrid.



Chapter 4

Analysis, Design and Realization of Broadband Bandpass Filters with Wide Upper Stopband Using Parallel-Coupled VIPSIRs and SSSIRs



4.1 Literature Survey

High performance wideband RF/microwave bandpass filters which need both broad passband and wide upper stopband are highly desirable for next generation broadband wireless communication systems. In the mean time, the conventional multi-layer printed circuit board (PCB) filter which uses low-cost FR4 or PTFE substrate (dielectric constant usually lower than 4.47) with a standard PCB process and requires no metal enclosure is also essential for cost reduction and mass productivity.

Considering the low cost PCB filters, although excellent performance has been achieved in conventional RF/microwave filters [1] such as parallel-coupled-line filters, interdigital filters, and comb-line filters, their fractional bandwidth can hardly exceed 50% due to the limitation on realizing tightly coupled lines especially the first and last coupling stages of the broadband filters. Recently, several works have solved the challenge of achieving wide bandwidth with several distinctive approaches such as a dual-mode ring resonator with tuning stubs [16-18], adding a third line in the parallel coupled line to obtain the tight coupling [19], distributed highpass filters with shunt short-circuit stubs [20], cascaded broadside-coupled structure [21], cascade or composite of low pass filters and highpass filters [22-25], and adoption of a multiple-mode resonator [26-29]. Most of the mentioned works can achieve a

filter with bandwidth more than an octave and some of them can be implemented by conventional PCB. However, none of them deal with the presence of spurious passbands which normally occur at $2f_0$, $3f_0$ or even $4f_0$. The presence of these spurious passbands causes poor upper stopband clearance or poor selectivity performance.

A well-known method to eliminate the spurious passband is to compensate the modal phase constant near the spurious passband frequency. Many published works based on this theory have been carried out by meandering the coupled line [30], adding compensation capacitors [31-32], and applying wiggly-coupled structures [33]. However, compensation of the modal phase constant over a wide frequency range is so difficult that only a specific harmonic passband, $2f_0$ for example, can be eliminated [30-32] or it is only valid for narrow band filter [33]. Another spurious passband eliminating method to use transmission zeros at spurious passband frequencies is also effective for narrowband filters but not for broadband filters. Because the spurious passband of a broadband filter is also wideband, a notch-like transmission zero can not suppress such a wideband spurious response. Broadband bandpass filters can also be designed using S-plane highpass or bandpass prototype under Richards transformation [34, 35]. In [34], applying the S-plane highpass prototype can implement a bandpass filter with very broad passband but its upper stopband is not separately controlled. In [35], two broadband bandpass filters with wide stopband clearance have been derived from S-plane bandpass prototypes with specific transmission zero locations using Richards transformation. The implementation of these filters is costly and the assembling process is complicated because a precisely fabricated mechanical enclosure to support the stripline is essential and an extra bounding equipment to construct the series lump capacitors is demanded.

As the filter bandwidth gets wider, the spurious passband becomes wide accordingly such that the space of the upper stopband is then squeezed. Therefore, pushing the spurious passband as far as possible from the main passband is essential especially for a broadband filter. A stepped impedance resonator (SIR) [8] has the property of moving the first spurious resonance away from twice of the fundamental resonant frequency. Several researches [36-38] have demonstrated very good performance of stopband clearance by pushing the spurious passband away from main passband. However, none of the proposed structures are applicable to a broadband filter due to their weak coupling strength. In order to push the first spurious resonance as far as possible, the impedance ratio R ($R=Z_{0H}/Z_{0L}$) of a stepped impedance resonator should be as high as possible where Z_{0H} and Z_{0L} are the characteristic impedance of high impedance and low impedance line sections, respectively. As the impedance ratio increases, the resonator length decreases. As a result, to achieve enough coupling for a broadband filter becomes more difficult. Therefore, special structures should be developed to solve mentioned problems. To the best of the author's knowledge, no published works have been reported to realize a broadband filter using stepped impedance resonator with very high impedance ratio.

In this dissertation, we propose two filter structures depicted in chapter 1 that one uses the vertically installed planar stepped impedance resonators (VIPSIRs), and the other uses the suspended substrate stripline stepped impedance resonators (SSSIRs). Both structures can solve the tight coupling problem for a broad passband and a high impedance ratio for extremely wide upper stopband clearance. Six filters, four (two) of them using VIPSIR (SSSIR), have been realized with more than an octave bandwidth and farther than $5f_0$ of the first spurious passband.

4.2 Filter Design Procedures

The design procedures for the parallel-coupled filter with relative narrow bandwidth are well documented in [1], also the approximate design and synthesis formulas are well developed for determining the even-and-odd mode impedances (Z_{0e} , Z_{0o}) of each coupled stages. As the filter's fractional bandwidth becomes larger, however, the accuracy of the synthesis formulas is limited by the frequency-dependent behavior of the J-inverter in the equivalent two-port network that is detailed in [39]. A corrective formula has been proposed by J. -T. Kuo [40] to compensate the frequency dependent behavior of the J-inverter. However, the accuracy decays drastically as the fractional bandwidth gets larger than 50%.

G. L. Matthaei [41] combined the image impedance and insertion-loss point of view to carry out the filter synthesis formulas that are applicable to filter with narrow and wide bandwidth. But the applications of the formulas are limited such that the electrical length of each coupled stages must be 90 degrees at the center frequency. Due to strong frequency dependence and non-90 degrees electrical length of coupled stage in proposed SIR filters, the filter design formulas mentioned above are not applicable to our case.

However, an optimization process in commercial circuit simulation tools such as Agilent ADS or AWR Microwave Office can do the task easily to obtain the even- and odd-mode characteristic impedances (Z_{0e} , Z_{0o}) of each coupled stage.

Therefore, the design procedures of the proposed parallel-coupled SIR filters of both structure A and B can be summarized as following.

- 1) Select an impedance value for the uncoupled high impedance line sections, and choose an appropriate electrical length (in our examples $1/12\lambda$ was chosen as an initial value).
- 2) According to the specification of the filter, utilize optimization tools in the circuit simulator to obtain the even- and odd-mode characteristic impedances (Z_{0e} , Z_{0o}) of each coupled stage without considering of the effect of open end and step junction fringing capacitors.
- 3) Use the design charts (Fig. 2.7-2.9 or Fig. 2.11-2.13) to acquire the corresponding physical dimensions.

- 4) Extract the values of fringing capacitance corresponding to the physical dimensions obtained in step (3).
- 5) Add the fringing capacitors and retune the length of coupled-line section.
- 6) Apply EM simulator to verify the performance of the filter and fine-tune it if necessary.

If the performance after the optimization procedure described in (2) did not get the target specification, procedure (1) should be conducted again with a revised impedance value. As we already know that the higher impedance values of the uncoupled line will move the spurious passband farther away from the passband. Besides, the selection of impedance value for each high impedance uncoupled line could be different that provides an extra degree of freedom during optimization.

Since the highly inhomogeneous properties of proposed structures, a set of initial values of even- and odd-mode effective dielectric constants ϵ_{ree} and ϵ_{reo} should be applied during execution of procedure (2) to obtain a temporary set of Z_{0e} , Z_{0o} and physical length of each coupled-line stage. After obtaining the values of Z_{0e} and Z_{0o} for each coupled-line section in the procedure (2), the corresponding dimension and effective dielectric constant ϵ_{ree} and ϵ_{reo} could be acquired from Figs. 2.7-2.9 or Figs. 2.11-2.13. If the acquired values of ϵ_{ree} and ϵ_{reo} in procedure (3) are not consistent with the initial given in procedure (2), an iterative process is necessary by replacing the initial values of ϵ_{ree} and ϵ_{reo} in procedure (2) with the newly acquired values. The iteration could be terminated until the values of ϵ_{ree} and ϵ_{reo} converge to the final values. Fortunately, it takes only two or three iterations to converge because the performances of the proposed filters are insensitive to the variation of effective dielectric constant. An important feature should be mentioned that for a set of given (Z_{0e}, Z_{0o}) values there have many different selections of the W_{LZ} and W in structure A or G_{gnd} and W in structure B. To choose these dimensions as large as possible is a good guideline because the modal impedance Z_{0e}/Z_{0o} varies rapidly as these dimensions are small.

Before executing procedure (5), the open-end and step-junction fringing capacitance values of each coupled-line sections should be extracted. The extraction of fringing capacitance values can be done easily by computer optimization where the fringing capacitors correlate the scattering parameters of the circuit model and the result from EM simulation. In our proposed filter structures, the step-junction capacitance could be considered to be the same as the open-end capacitance due to the large abrupt change on the junction width. The fringing capacitors of each section could be extracted separately, thus, the efforts of EM simulation and circuit extraction could be reduced. While considering the fringing capacitors, the physical length of each coupled-line section should be shortened. Therefore, in procedure (5), apply the fringing capacitors to the circuit model and redo the procedure (2) to obtain the new length of each coupled-line section.

In the end, the desired filter's physical dimensions can be obtained easily and fast with the help of the circuit simulation model and the design charts. It confirms very well to the

results obtained by time-consuming EM simulation. In the next section, several ultra-broadband filters with outstanding upper stopband suppression performance will be designed, fabricated and measured to demonstrate the validity of the proposed design procedures.

4.3 Simulation and Measurement

4.3.1 The VIPSIR Filters

Four VIPSIR filters (A,B,C,D) were fabricated and measured to demonstrate the validity of design procedure for ultra-wideband filter. The specifications and structural parameters of the filters are listed in Table 4.1 where i represent the sequential number for the composing elements shown in the circuit model. As presented in Fig. 2.5, for example, an equivalent circuit model of a third-order filter comprises seven circuit elements. Due to the symmetrical property of the filter, the parameters for the i -th section are same as $(2N+2-i)$ -th section where N is the order of the filter. There are two kinds of information provided for a VIP coupled-line section. One is the parameters in circuit model obtained by optimization procedures and the other is the corresponding physical dimensions gotten from the design charts. The rest of the physical parameters such as H_{sub} , ϵ_{rl} , ϵ_{r2} , W_{HZ} , and H_{VIP} for the designed filters are demonstrated in Fig. 2.6.

In the following experimental examples, a substrate material, Roger RO4003 with $\epsilon_r=3.38$, is applied to both the VIP and the main substrate but the substrate thicknesses are 0.2032mm (8mils) for VIP and 0.508mm (20 mils) for main substrate respectively.

Table 4.1 Specifications and dimensions of the experimental filters of structure A

Filters	Order	FBW %	Coupled line sections								High impedance Lines			
			Section	Parameters in circuit model				Dimension (mm)			Section	Ohm	mm	mm
				$Z_{0e}(\Omega)$	ϵ_{ree}	$Z_{0o}(\Omega)$	ϵ_{reo}	W	W_{LZ}	ℓ		Z_{0H}	D_{HZ}	ℓ
A	$N=3$	70%	$i=1$	130.6	1.750	8.06	3.16	0	2.286	5.334	$i=2$	198.5	1.52	3.5814
			$i=3$	57.55	2.761	8.06	3.21	1.143	2.032	5.029	$i=4$	198.5		5.08
B	$N=5$	70%	$i=1$	130.6	1.750	8.06	3.16	0	2.286	5.842	$i=2$	185	1.27	3.429
			$i=3$	66.6	2.7	8.6	3.21	0.940	1.905	5.461	$i=4$	185		5.2832
			$i=5$	62	2.81	11.6	3.17	1.041	1.27	5.334	$i=6$	185		5.588
C	$N=5$	70%	$i=1$	105	2.2	8.2	3.19	0.178	2.159	6.731	$i=2$	173	1.01	3.7338
			$i=3$	58	2.74	8.1	3.21	1.092	2.032	5.207	$i=4$	173		5.7658
			$i=5$	66	2.76	13.7	3.14	0.940	1.016	5.765	$i=6$	106		5.334
D	All dimensions are same as filter C but arrange in different manner.													

Fig. 4.1 and Fig. 4.2 show the simulated and measured responses of filter A and B where the orders of the filters are 3 and 5 respectively. Filter A and B are Chebyshev-response filters with 0.1-dB passband ripple level. Both filters have $f_0=3\text{GHz}$, 70% fractional bandwidth (FBW), and wide upper stopband clearance performance (up to $5f_0$). It is observed that not only the first spurious passband is pushed up to $5f_0$ but also better than -30dB for filter A and -40dB for filter B of rejection level are achieved in the whole upper stopband. The pass band return loss of filter A is better than -17dB and that of filter B is better than -15dB . Moreover, there are three sets of data shown in Fig. 4.1 and Fig. 4.2. Respectively, the broken lines depict the simulated results by circuit model, the bold lines represent the EM simulation results and the bold lines with symbols on it describe the measured responses. The measured data of the filters match very well with that obtained by both circuit model and EM simulation, which verifies that the circuit model could provide very good accuracy.

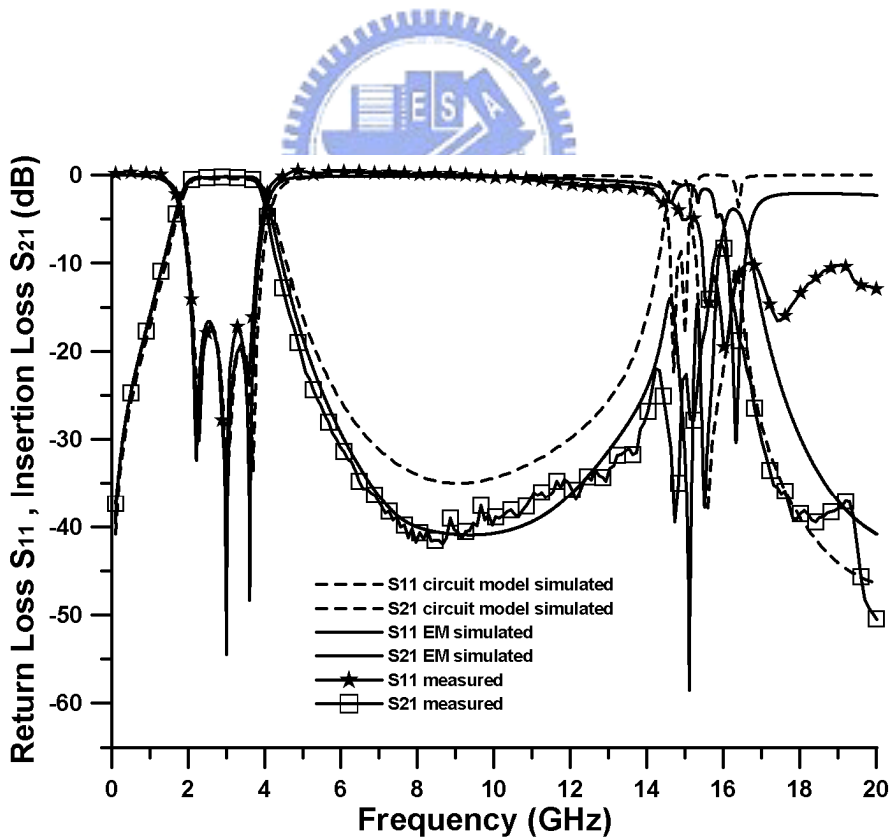


Fig. 4.1 Simulated and measured responses of filter A.

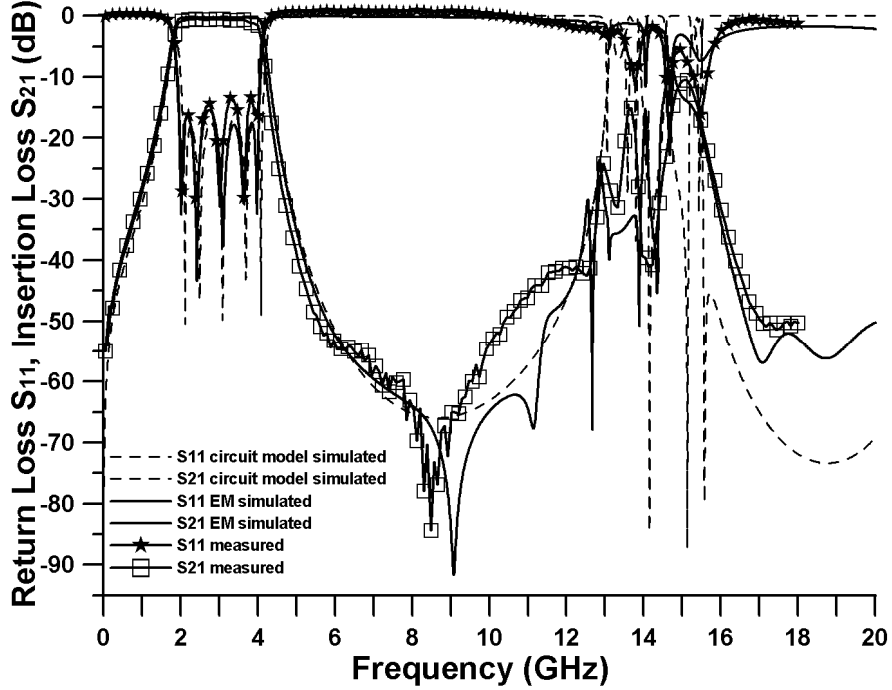


Fig. 4.2 Simulated and measured responses of filter B

In filters A and B, the impedances of the VIP high-impedance lines are chosen to be equal. In filter C, we choose the central section; the section number sixth, has different impedance than others. A 0.254mm (10mils) microstrip transmission line on the main substrate is applied at the middle of the filter C to connect two pieces of VIP substrates, which are placed in a straight manner to compare the performance with filter D. The filter D as illustrated in Fig. 4.3 is the folded version of filter C. The size of filter D is reduced as comparing with that of filter C.

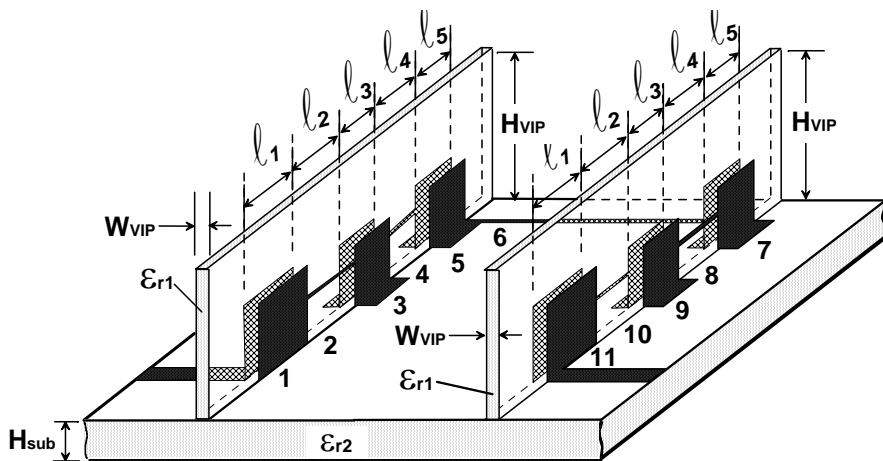


Fig. 4.3 A sketch drawing for filter D. A high impedance microstrip line is used to connect two VIP substrates. The numbers on the mail substrate indicate the section number in Table 4.1.

Fig. 4.4 depicts the simulated and measured results of filter C, whose designed response is Chebyshev type of 0.1-dB passband ripple level. The center frequency and FBW of filter C were 3GHz and 70% respectively. The third resonator with high impedance microstrip line could only push its second resonant frequency to 9.3GHz due to its lower impedance ratio ($R=Z_{0H} / Z_{0L}$) comparing to the other resonators. This causes an insertion loss peak located around 9.3 GHz. In spite of the insertion loss peak, the first spurious pass band of the filter C is pushed up to $4.5f_0$ and approximately a -30dB rejection level in the upper stopband is obtained.

The simulation and measured results of filter D are shown in Fig. 4.5. Filter D has same filter specification and physical dimensions as filter C. As shown in Fig. 4.3, we fold the filter to reduce size. Because the folding geometry generates a cross coupling between resonator 1 and 5, the insertion loss peak around 9.3GHz is eliminated. Therefore, the space saving layout of filter D can achieve similar upper stopband clearance as filter B. The photographs of fabricated filter A and B are depicted in Fig. 4.6 (a) and (b) respectively.

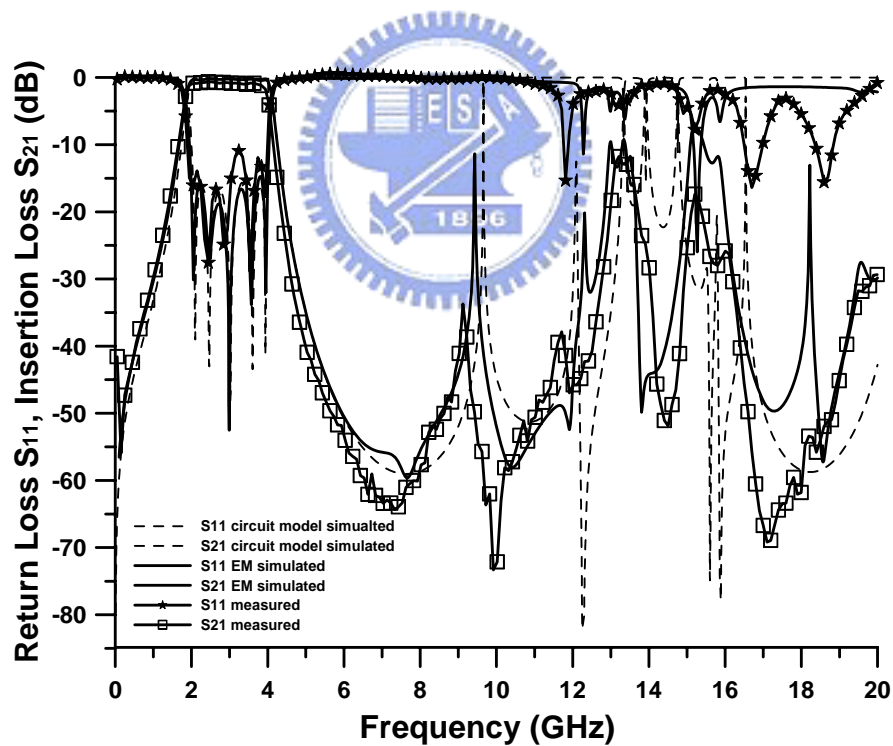


Fig. 4.4 Simulated and measured responses for filter C.

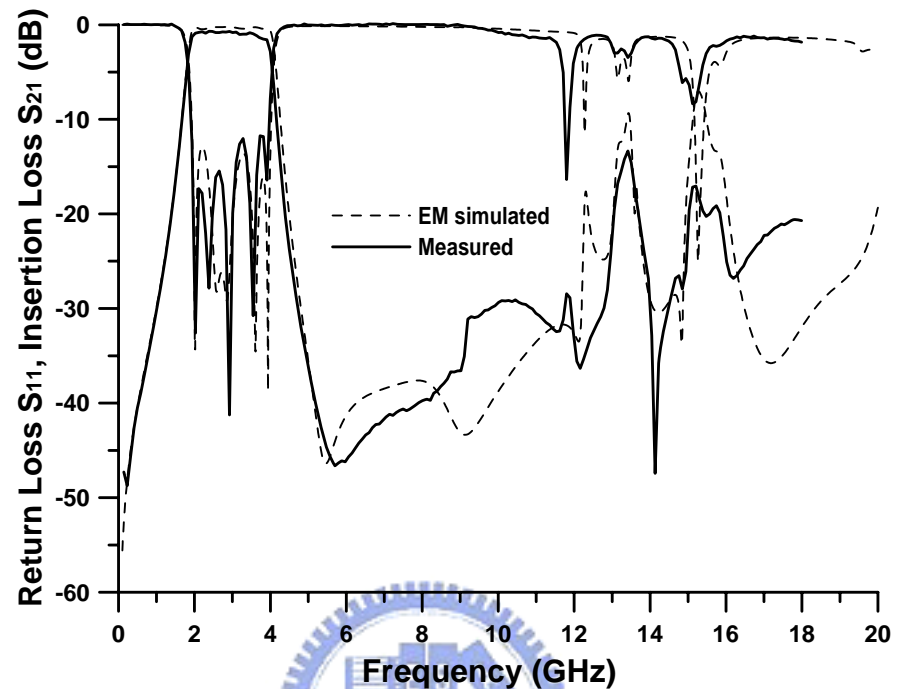


Fig. 4.5 Simulated and measured responses for filter D.

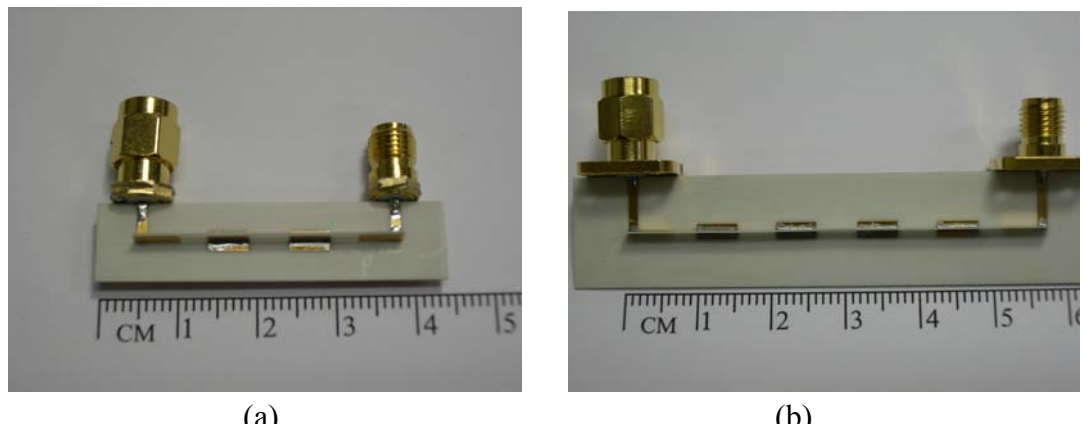
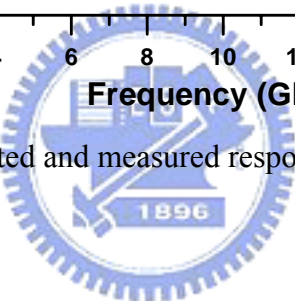


Fig. 4.6 Photographs of proposed (a) filter A and (b) filter B.

4.3.2 The SSSSIR Filters

In this section, two design examples of broadband bandpass filters using SSSSIRs are presented. The filters are fabricated and measured to demonstrate the validity of design procedures and the outstanding stopband performance. The specifications and structural parameters of the filters are listed in Table 4.2, where i represent the sequential number for the composing elements shown in the circuit model. The extracted fringing capacitance values of each capacitor are listed at the bottom of Table 4.2. In these experimental examples a substrate material, Rogers RO4003 with $\epsilon_r=3.38$, is applied to each layer.

Table 4.2 Specifications and dimensions of the experimental filters of Filter structure B

Filters	Order	FBW%	Coupled line sections							High impedance Lines				
			Section	Parameters in circuit model				Dimension (mm)			Section	Ohm	mm	mm
				$Z_{0e}(\Omega)$	c_{ree}	$Z_{0o}(\Omega)$	c_{reo}	W	G_{gnd}	ℓ		Z_{0H}	G_{gnd}	ℓ
E	$N=3$	70%	$i=1$	128	2.189	7.6	3.32	2.286	4.064	4.572	$i=2$	202	7.366	3.175
			$i=3$	51	3.08	7.95	3.33	2.032	1.27	3.81	$i=4$	202		4.749
F	$N=5$	70%	$i=1$	128	2.189	7.6	3.31	2.286	4.064	5.461	$i=2$	202	7.366	2.921
			$i=3$	54	3	7.9	3.32	2.032	1.397	4.114	$i=4$	202		4.826
			$i=5$	49	3.24	8.9	3.35	1.778	0.762	3.81	$i=6$	202		4.953

Fringing Capacitors in Filter E: $C_{01}=0.18\text{pF}$, $C_{12}=0.025\text{pF}$, $C_{23}=C_{34}=0.05\text{pF}$

Fringing Capacitors in Filter F: $C_{01}=0.18\text{pF}$, $C_{12}=0.025\text{pF}$, $C_{23}=0.045\text{pF}$, $C_{34}=C_{45}=0.045\text{pF}$

Fig. 4.7 and Fig. 4.8 depict the simulated and measured results of filter E and F. The filter E is a third-order Chebyshev filter with 0.15dB of passband ripple, 3GHz of center frequency f_0 , and 70% of fractional bandwidth. The filter F is a fifth-order Chebyshev filter with same electrical parameters as filter A except its passband ripple to be 0.1dB.

It can be observed in Fig. 4.7 and Fig. 4.8 that the spurious passband are pushed up to more than $5f_0$. Moreover, better than -30dB for filter A and -40dB for filter B stopband rejection level are achieved. Again, each figure contains three different data that are acquired by circuit model, EM simulation, and experimental measurement respectively. Both filters show good agreement between these three data. The photographs of fabricated filter E and F are depicted in Fig. 4.9 (a) and (b) respectively.

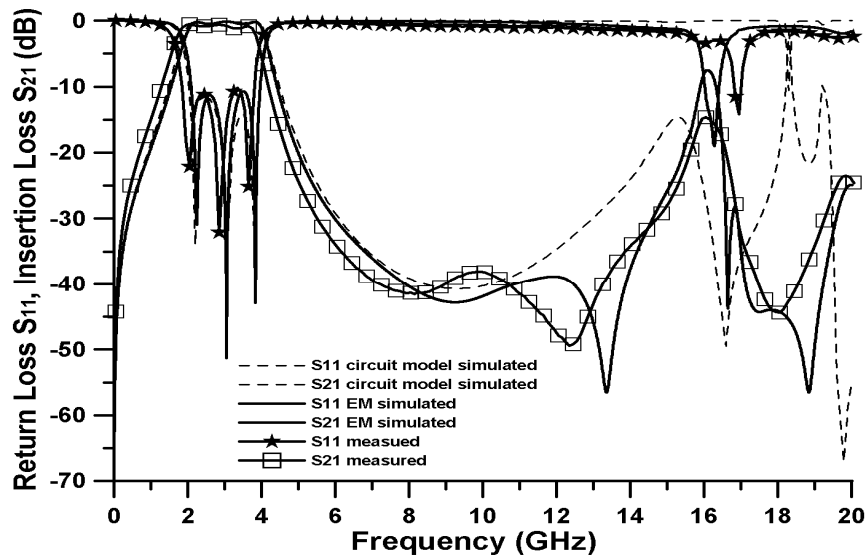


Fig. 4.7 Simulated and measured responses of filter A.

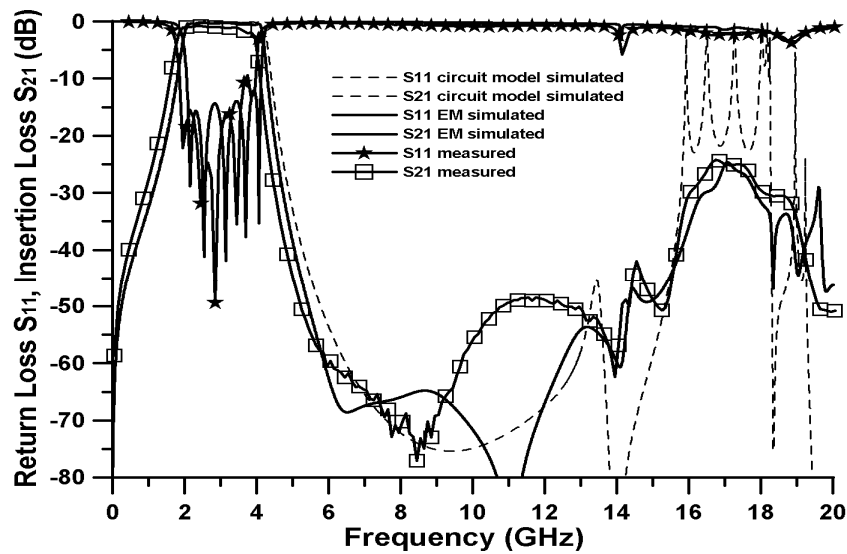


Fig. 4.8 Simulated and measured responses of filter B.

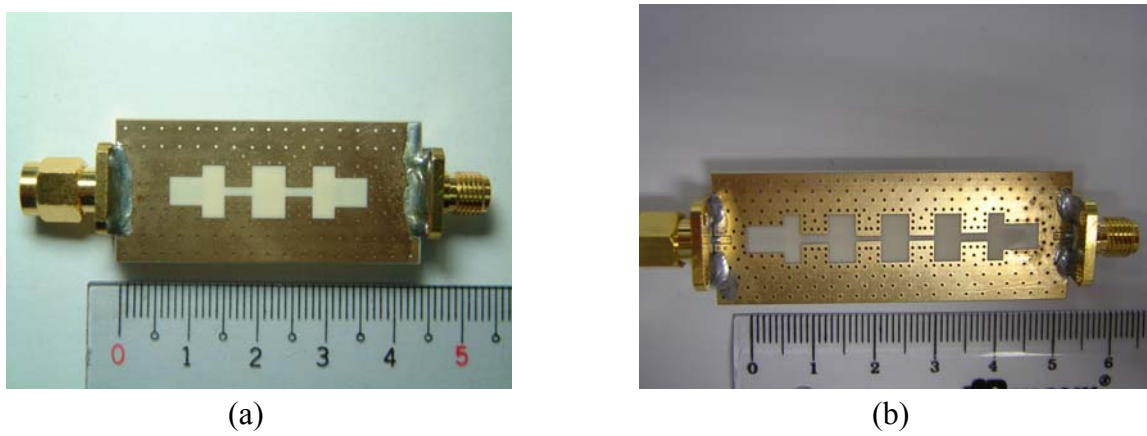
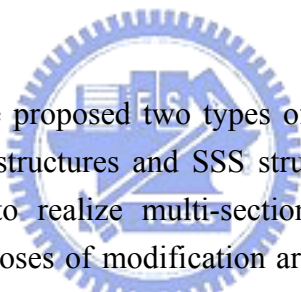


Fig. 4.9 Photographs of fabricated (a) filter E and (b) filter F.

Chapter 5

Conclusions



In this dissertation, we have proposed two types of three-dimensional extremely tight coupling structures, namely VIP structures and SSS structure. Two modified VIP coupling structures have been proposed to realize multi-section cascade quadrature hybrid with multi-octave bandwidth. The purposes of modification are to compensate the unequal modal phase velocities, to further increase the coupling to as tight as -0.8 dB, and to provide layout freedom of minimizing the discontinuity effect. The proposed structure type I not only can compensate the unequal modal phase velocity but also provide the flexibility of physical layout to minimize the junction effect that occurred between different coupled-line sections. However, the proposed type I coupling structure can not provide an extremely tight coupling as tight as -0.8dB and that is necessary when realize a quadrature hybrid with multi-octave bandwidth. Therefore, the type II coupling structure has been successfully proposed to achieve an extremely tight coupling by adopting the ground aperture technique. Both coupling structures use dielectric blocks beside the vertically substrate to compensate the modal phase velocities over a wide frequency range. Moreover, the vertically substrate and the main substrate in proposed coupling structure can be the low dielectric constant PCB substrates where the conventional PCB etching and assembly process can be used for mass production. Following the systematical design procedures accompany with the design charts, a design example of a five-section quadrature hybrid with passband ripple of +/- 0.5dB and frequency range of 1-9GHz is realized. The measured amplitude imbalance is less than +/-0.65dB and phase difference is keeping at 90° +/- 5° over the designed frequency of 1-9GHz. The experimental data confirm very well with the simulation result to demonstrate the validation

of proposed structure and design procedures.

For a broadband filter, the extremely tight coupling structure is also an essential circuit element. Fortunately, the unequal modal phase velocities could not be a problem for filter application because filter is not sensitive to phase velocity difference. Therefore, the conventional VIP coupler can be used. Moreover, we have proposed a modified stripline structure with ground plane opening. The modified structure has been named as SSS structure. Similar to the conventional VIP coupled-line structure, the SSS coupled-line structure is also suitable for broadband filter application.

Besides the tightly coupled line portion, an extremely high impedance uncoupled line is required to implement a SIR filter. Fortunately, both conventional VIP and SSS structures can realize an extremely high impedance uncoupled lines.

Therefore, two filter structures using VIPSIRs and SSSSIRs are proposed to realize bandpass filters with a bandwidth of broader than 1:2, and a wide and good upper stopband suppression. Same as multi-section coupler, the two proposed filter structures are both suitable for standard PCB process and low cost low dielectric constant material. Both proposed filter structures can realize extremely low impedance values of coupled line section and really high impedance values of un-coupled transmission line section. Therefore, a SIR with very high impedance ratio R ($R=Z_{0H}/Z_{0L}$) can be realized. As a result, the harmonic passband could be pushed far away from the passband and a wide and good upper stopband clearance could be achieved. Several experimental examples using proposed filter structure have been designed and fabricated. The fractional bandwidth of the designed examples can be as wide as 70% and the nearest harmonic passband of most cases are located more than $5f_0$. Excellent upper stopband suppression (better than -30dB and -40dB suppression for three and five order filter respectively) has been accomplished. Systematic, fast, and accurate filter design procedures using commercial circuit simulator accompany with the design charts have been introduced. Again, the experimental data confirm very well with the simulation results to demonstrate the validation of proposed structure and design procedure.

Proposed three-dimensional coupling structure not only can apply to quadrature coupler and filter design. In the future work, the proposed coupling structures also can also be used in different RF/microwave circuits such as broadband balanced mixer, broadband balun, and balanced amplifiers. Moreover, the vertically installed planar configuration can be a good solution for the circuit crossover problem between two arms of microstrip lines. For example, two modified rat-race rings can be cascaded together to form an interesting performance [42]. In the modified rat-race ring a VIP cross-over is used. We believe that more study could be done on this kind of circuit where a cross-over is required for the implementation of the circuit.

Reference

- [1] G. L. Matthaei, L. Young, and E. M. T. Jones *Microwave Filters, Impedance matching Networks and Coupling Structures*, Norwood, MA: Artech House, 1980.
- [2] S. B. Cohn, "The re-entrant cross section and wide-band 3-dB hybrid couplers," *IEEE Trans. Microwave Theory Tech.*, vol. 11, no. 4, pp. 254-258, Jul. 1963.
- [3] J. Lange, "Interdigitated stripline quadrature hybrid," *IEEE Trans. Microwave Theory Tech.*, vol. 17, no. 12, pp. 1150-1151, Dec. 1969.
- [4] Bhartia, P. and P. Pramanick, "Computer-aided design models for broadside-coupled striplines and millimeter-wave suspended substrate microstrip lines," *IEEE Trans. Microwave Theory Tech.*, vol. 36, pp.1476-1481, Nov. 1988.
- [5] Cohn, S. B. and R. Levy, "History of microwave passive components with particular attention to directional couplers," *IEEE Trans. Microwave Theory Tech.*, vol. 32, no. 9, pp. 1046-1054, Sept. 1984.
- [6] Y. Konishi, I. Awai, Y. Fukuka, and M. Nakajima, "A directional coupler of a vertically installed planar circuit structure," *IEEE Trans. Microwave Theory Tech.*, vol. 36, no. 6, pp.1057-1063, June 1988.
- [7] C. Zhao and I. Awai, "Application of the finite difference techniques to the compensated VIP 3 dB directional coupler," *IEEE Trans. Microwave Theory Tech.*, vol. 44, no. 11, pp. 2045-2052, Nov. 1996.
- [8] M. Makimoto, and S. Yamashita, "Bandpass filters using parallel coupled stripline stepped impedance resonators," *IEEE Trans. Microwave Theory Tech.*, vol. 28, no. 12, pp. 1413-1417, Dec. 1980.
- [9] I. Awai and C. Zhao, "Analysis of vertically installed planar (VIP) combline bandpass filters," in *Asia-Pacific Conference Proceedings*, Dec.1997, vol.2, pp.801-804.
- [10] S. L. March, "Phase velocity compensation in parallel-coupled microstrip," in *IEEE MTT-S Int. Microwave Symp. Dig.*, Jun 1982, vol. 82, no. 1, pp.410-412.
- [11] S. B. Cohn, "The re-entrant cross section and wide-band 3-dB hybrid couplers," *IEEE Trans. Microwave Theory Tech.*, vol. 11, no. 4, pp. 254-258, Jul. 1963.
- [12] B. Sheleg and B. E. Spielman, "Broad-band directional couplers using microstrip with dielectric overlays," *IEEE Trans. Microwave Theory Tech.*, vol. 22, no. 12, pp. 1216-1220, Dec. 1974.
- [13] C. Buntschuh, "High directivity microstrip couplers using dielectric overlays," in *IEEE MTT-S Int. Microwave Symp. Dig.*, May 1975, vol. 75, no. 1, pp.125-128.
- [14] Klein, J. L. and K. Chang, "Optimum dielectric overlay thickness for equal even- and odd- mode phase velocities in coupled microstrip circuits", *Electronics Letters*, vol. 26, no. 5, pp. 274-276, March 1990.

[15] E. G. Cristal and L. Young, "Theory and tables of optimum symmetrical TEM-mode coupled transmission line directional couplers", *IEEE Trans. Microwave Theory Tech.*, vol. 13, no. 5, pp. 544-558, Sept. 1965.

[16] H. Ishida and K. Araki, "Design and analysis of UWB band pass filter with ring filter," in *IEEE MTT-S Int. Microwave Symp. Dig.*, June 2004, vol. 3, pp. 1307–1310.

[17] L.-H. Hsieh and K. Chang, "Compact, low insertion-loss, sharp-rejection, and wide-band microstrip bandpass filters," *IEEE Trans. Microwave Theory Tech.*, vol. 51, no. 4, pp. 1241–1246, Part 1, April 2003.

[18] J. Konpang, A. Namahoot, and P. Akkaraekthalin, "A wide-band bandpass filter using properties of microstrip open-loop resonators with outer tuning stubs," in *TENCON 2004. 2004 IEEE Region 10 Conference*, Nov. 2004, vol. 3, pp. 624–627.

[19] J.-T. Kuo and E. Shih, "Wideband bandpass filter design with three-line microstrip structures," *IEE Proceedings on Microwaves, Antennas and Propagation*, vol. 149, pp. 243–247, Oct.-Nov. 2002.

[20] Y.-S. Lin, W.-C. Ku, C.-H. Wang, and C. H. Chen, "Highly selective microstrip bandpass filters for ultra-wideband (UWB) application," in *Asia-Pacific Conference Proceedings*, Dec. 2005, vol. 5, pp. 4-7.

[21] K. Li, D. Kurita, and T. Matsui, "An ultra-wideband bandpass filter using broadside-coupled microstrip-coplanar waveguide structure," in *IEEE MTT-S Int. Microwave Symp Dig.*, June 2005, vol.12-17, pp. 675–678.

[22] C.-L. Hsu, F.-C. Hsu, and J.-T. Kuo, "Microstrip bandpass filters for ultra-wideband (UWB) wireless communications," in *IEEE MTT-S Int. Microwave Symp Dig.*, Jun 2005, vol.12-17, pp. 679-682.

[23] Y.-S. Lin, W.-C. Ku, C.-H. Wang, and C. H. Chen, "Wideband coplanar-waveguide bandpass filters with good stopband rejection," *IEEE Microwave and Wireless Components Letters*, vol.14, no. 9, pp. 422 – 424, Sept. 2004.

[24] T.-N. Kuo, S.-C. Lin, and C. H. Chen, "Compact ultra-wideband bandpass filters using composite microstrip-coplanar-waveguide structure," *IEEE Transactions on Microwave Theory Tech.*, vol.54, pp. 3772-3778, Oct. 2006.

[25] W. Menzel, T. Rahman M. S., and L. Zhu, "Low-loss ultra-wideband (UWB) filters using suspended stripline," in *Asia-Pacific Conference Proceedings*, Dec. 2005, vol. 4, pp. 4-7.

[26] W. Menzel, L. Zhu, K. Wu, and F. Bogelsack, "On the design of novel compact broad-band planar filters," *IEEE Transactions Microwave Theory Tech.* vol. 51, no. 2, pp. 364-370, Feb. 2003.

[27] Y.-C. Chiou, J.-T. Kuo, and E. Cheng, "Broadband quasi-Chebyshev bandpass filters with multimode stepped-impedance resonators (SIRs)," *IEEE Transactions Microwave Theory Tech.*, vol. 54, no.8, pp. 3352–3358, Aug. 2006.

[28] L. Zhu, H. Bu, and K. Wu, "Broadband and compact multi-pole microstrip bandpass filters using ground plane aperture technique," *IEE Proceedings on Microwaves, Antennas and Propagation*, vol. 149, no. 1, pp. 71-77, Feb. 2002.

[29] S. Sun, and L. Zhu, "Capacitive-ended interdigital coupled lines for UWB bandpass filters with improved out-of-band performances," *IEEE Microwave and Wireless Components Letters*, vol. 16, no. 8, pp. 440–442, Aug. 2006.

[30] S.-M. Wang, C.-H. Chi, M.-Y. Hsieh, and C.-Y. Chang, "Miniaturized spurious passband suppression microstrip filter using meandered parallel coupled lines," *IEEE Trans. Microwave Theory Tech.*, vol. 53, no. 2, pp. 747-753, Feb. 2005.

[31] S. L. March, "Phase velocity compensation in parallel-coupled microstrip," in *IEEE MTT-S Int. Microwave Symp. Dig.*, Dec. 1982, vol. 82, no. 1, pp. 410-412.

[32] I. J. Bahl, "Capacitively compensated high performance parallel coupled microstrip filters," in *IEEE MTT-S Int. Microwave Symp. Dig.*, Jan. 1989, vol. 2, pp. 679-682.

[33] T. Lopetegi, M. A. G. Laso, J. Hernandez, M. Bacaicoa, D. Benito, M. J. Garde, M. Sorolla, and M. Guglielmi, "New microstrip 'wiggly-line' filters with spurious passband suppression," *IEEE Trans. Microwave Theory Tech.*, vol. 49, no. 9, pp. 1593-1598, Sept. 2001.

[34] R. Levy, "New equivalent circuits for inhomogeneous coupled lines with synthesis applications," *IEEE Trans. Microwave Theory Tech.*, vol. 36, no. 6, pp. 1087-1094, June 1988.

[35] B. J. Minnis, "Class of sub-miniature microwave printed circuit filters with arbitrary passband and stopband widths," *IEEE Trans. Microwave Theory Tech.*, vol. 82, no. 11, pp. 1893-1900, Nov. 1982.

[36] M. Makimoto and S. Yamashita, "Bandpass filters using parallel coupled stripline stepped impedance resonators," *IEEE Trans. Microwave Theory Tech.*, vol. 28, no. 12, pp. 1413-1417, Dec. 1980.

[37] H.-K. Pang, K.-M. Ho, K.-W. Tam and R.P. Martins, "A compact microstrip $\lambda/4$ -SIR interdigital bandpass filter with extended stopband," in *IEEE MTT-S Int. Microwave Symp. Dig.*, June 2004, vol. 3, pp. 1621-1624.

[38] J.-T. Kuo and E. Shih, "Microstrip stepped impedance resonator bandpass filter with an extened optimal rejection bandwidth," *IEEE Trans. Microwave Theory Tech.*, vol. 51, no. 5, pp. 1554-1559, May 2003.

[39] S. B. Cohn, "Parallel-coupled transmission-line-resonator filters," *IRE Trans. on Microwave Theory Tech.*, vol. 6, no. 2, pp. 223-231, Apr. 1958.

[40] K.-S. Chin, L.-Y. Lin, and J.-T. Kuo, "New formulas for synthesizing microstrip bandpass filters with relatively wide bandwidths," *IEEE Microwave and Wireless Components Letters*, vol. 14 , no. 5, pp. 231 – 233, May 2004.

[41] G. L. Matthaei, "Design of wide-band (and narrow-band) band-pass microwave filters on the insertion loss basis," *IRE Trans. on Microwave Theory Tech.*, vol. 8, no. 6, pp.580-593, Nov. 1960.

[42] C.-H. Chi, and C.-Y. Chang, "A wideband bandpass filter with wide upper stopband using stepped-impedance cascadable 180° hybrid rings," *IEEE Microwave and Wireless Components Letters*, vol. 17, no. 8, pp. 589-591, Aug. 2007.



博士候選人資料

姓 名 : 陳慧諄

性 別 : 男

出生年月日 : 民國 60 年 04 月 08 日

籍 貫 : 台灣省彰化縣



學 歷 : 私立元智大學電機工程學系畢業(79 年 9 月~83 年 6 月)

私立大葉大學電機研究所畢業 (83 年 9 月~85 年 6 月)

國立交通大學電信研究所博士班(90 年 9 月~)

經 歷 : 正文股份有限公司研發部研發工程師 (87 年 6 月~90 年 6 月)

正文股份有限公司研發部研發副理 (90 年 6 月~94 年 6 月)

正文股份有限公司研發部研發經理 (94 年 6 月~)

論文題目 : 立體超緊耦合結構之研究與其在寬頻耦合器與和帶通濾波器

的應用

Publication List

Hui-Chun Chen

A. Journal paper

[1] H.-C. Chen and C.-Y. Chang, "Printed Circuit Board Bandpass Filters with Octave Bandwidth and Very Wide Upper Stopband," *Institute of Electronics, Information and Communication Engineers Transactions on Electronics*, vol. E90-C, no. 12, pp. 2205-2211, Dec. 2007.

[2] H.-C. Chen and C.-Y. Chang, "Modified VIP (vertically installed planar) couplers for ultra-broadband multi-section quadrature hybrid," *IEEE Microwave and Wireless Components Letters*, vol.16, no. 8, pp. 446-448, Aug. 2006.

B. Conference paper

[3] H.-C. Chen and C.-Y. Chang, "Suspended Substrate Stripline Bandpass Filters with both Broad Passband and Wide Upper Stopband," in *Asia-Pacific Conference Proceedings*, Dec. 2007, pp. 505-508.

